Ultrafast Dynamics of the Excited States of Curcumin in Solution

Rajib Ghosh, Jahur A. Mondal, and Dipak K. Palit*

Radiation & Photochemistry Division, Bhabha Atomic Research Centre, Trombay, Mumbai 400085, India

Received: April 28, 2010; Revised Manuscript Received: August 11, 2010

Dynamics of the excited singlet (S_1) state of curcumin has been investigated in a wide varieties of solvents using subpicosecond time-resolved fluorescence and absorption spectroscopic techniques. As a consequence of extra stability of the *cis*-enol conformer due to the presence of an intramolecular hydrogen bond, it is the major form existing in the ground-state and the excited-state processes described here has been attributed to this form. Steady-state absorption and fluorescence spectra suggest significant perturbation of the intramolecular hydrogen bond and the possibility of formation of intermolecular hydrogen-bonded complex with the hydrogen-bonding solvents. Both the time-resolved techniques used here reveal that solvation is the major process contributing to the relaxation dynamics of the S_1 state. Solvation dynamics in protic solvents is multimodal, and the linear correlation between the longest component of the solvation process and the longitudinal relaxation time of the solvent suggests the specific hydrogen-bonding interaction between the solute and the solvent. However, a good correlation between the experimentally determined average solvation time and that predicted by the dielectric continuum model in all kinds of solvents also suggests that the dielectric relaxation of the solvent is also an important contributor to the solvation process. The lifetime of the S_1 state is very short in nonpolar solvents (~44 ps in 1,4-dioxane) because of efficient nonradiative deactivation of the S_1 state, which is an important consequence of the ultrafast excited-state intramolecular hydrogen transfer (ESIHT) reaction in the six-membered hydrogen-bonded chelate ring of the *cis*-enol form. However, it has not been possible to monitor the ESIHT reaction in real time because of the symmetrical structure of the molecule with respect to the hydrogen-bonded chelate ring. In polar solvents, dipole−dipole interaction perturbs the intramolecular hydrogen bond leading to the reduced efficiency of the nonradiative deactivation process. However, stretching vibration in the intermolecular hydrogen bonds formed in the hydrogen-bonding (both donating and accepting) solvents induces another efficient channel for the nonradiative relaxation of the S_1 state of curcumin.

1. Introduction

Curcumin has been the subject of intense investigations in the wide ranging fields of physics, chemistry, biology, and medicine because of its potential applications as antioxidant, anti-inflammatory, and anticancer agents.[1–6] Curcumin has also been identified to have the ability to prevent protein aggregation in debilitating diseases such as Alzheimer's and Parkinson's.[7–10]

Structurally, curcumin is an α,β-unsaturated β-diketonic compound, in which two *o*-methoxyphenolic moieties are attached symmetrically through two π-conjugated ethylene linkers (Scheme 1). NMR, absorption, and fluorescence spectroscopic techniques have been widely employed to study the structural, photophysical, photobiological and biophysical properties of curcumin and its derivatives in solutions and in different kinds of heterogeneous media, such as micelles, vesicles and membranes.[11–25] Among several possible isomeric structures of curcumin, as proposed by Sun et al.[20] only three of them, which can be considered as candidates for the ground state of curcumin, are shown in Scheme 1. Structure I, which is the *cis*-diketo form, is the most common representation of curcumin. However, full geometry optimization starting with the *cis*-dikeo structure using high level ab initio computations performed by Balasubramanian did not produce a minimum but it rearranged to the *trans*-diketo form (structure II).[21] In addition, the *trans*-diketo isomer was found to be a minimum with all real vibrational frequencies by computation, confirming this as a potential isomer of curcumin.

SCHEME 1: Chemical Structures of the *cis*- and *trans*-Diketo Forms of Curcumin and the Keto−Enol Tautomeric Equilibrium

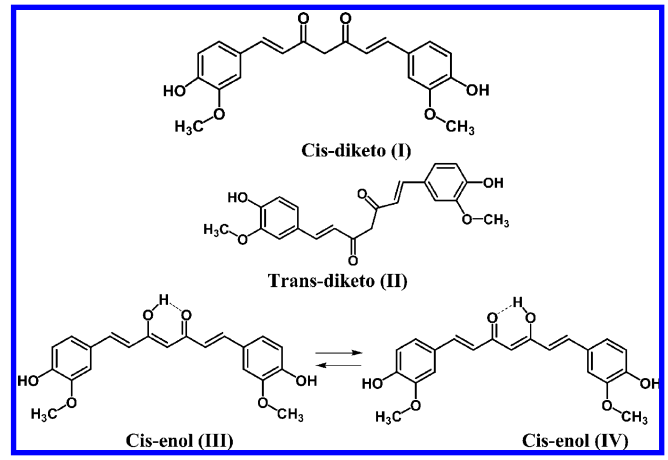

The reason for this isomerization was assigned to the negative charges on the C═O groups, which resulted in a strong electrostatic repulsion between the two C═O groups. Further, the ^{1}H and ^{13}C NMR and IR spectra of curcumin in chlorobenzene revealed that the *cis*-keto structure of curcumin undergoes a keto−enol rearrangement by transfer of a proton from the CH_2 group to form the enol form (structure III) and it is essentially the major conformer of this molecule present in a variety of solvents.[20] NMR experiments performed by several

* Corresponding author. E-mail: dkpalit@barc.gov.in. Tel: 91-22-25595091. Fax: 91-22-25505151.

10.1021/jp1038249
Published on Web 08/31/2010

other groups too established that the *cis*-enol form of curcumin is essentially the only form of this molecule present in a variety of solvents ranging from chloroform to mixtures of dimethyl sulfoxide (DMSO) and water with varying pH in the range 3−9.[21–26] Geometry optimization of the *cis*-enol structure at different levels of computational theories revealed that the enolic form with the dihedral angle of 180° was planar and was definitely the most stable form of the ground state both in the gas phase and in aqueous solution.[27–32] Theoretical calculations have also established the fact that the *cis*-enol form is more stable than the *cis*-diketo form, and the energy difference is about 7.75 kcal mol^{-1}.[28] Further, Balasubramanian also showed that the diketo structure exists only in the trans form and it is 6.7 and 6.9 kcal mol^{-1} above the enol form in the gas phase and solution, respectively. Formation of the *cis*-enol structure becomes preferred because of its large dipole moment (7.7 and 10.8 D in the gas and solution phases, respectively), which leads to formation of a strong intramolecular H-bond, as well as the extended conjugation of the molecular backbone compared with that of the diketo form.[27,28] Moreover, the TDDFT calculated absorption spectra and oscillator strengths of both isomers provide further evidence to support the conclusion that the enol form of curcumin predominates in solution. The experimental value of the absorption maximum for the enol form of curcumin (417 nm in benzene or 419 nm in chloroform) is very close to the calculated absorption maximum (419 nm), suggesting the predominance of this form in solution.[11–13,27,28] On the contrary, the structure of the diketo form is twisted and the theoretically predicted absorption maximum shifts to the near-ultraviolet region.[27,28] In fact, the *cis*-enol form may be considered as coexisting in two equivalent or symmetric keto−enol tautomers (structures III and IV), which may interconvert between each other via an intramolecular hydrogen atom transfer (IHT) process. NMR spectroscopic analysis in solution indicated only the presence of rapidly interconverting structures III and IV.[21]

Several studies have focused on the photophysical properties of the excited states of curcumin in different kinds of solvents using time-resolved fluorescence spectroscopy in pico- and subpicosecond time scales and have predicted about the occurrence of two fundamental photophysical processes of the excited state, namely the excited-state intramolecular hydrogen atom (or proton) transfer, ESIHT (or ESIPT) process, as well as dipolar solvation.[12–19] First, solvation is expected to play an important role in the excited-state relaxation dynamics of curcumin because of a significant change in the dipole moment ($\Delta\mu \sim 6.1$ D) following photoexcitation of the molecule from the ground electronic (S_0) state to the first excited singlet (S_1) state.[12] This value is comparable to that of Coumarin 153 ($\Delta\mu \approx 8$ D), which has been extensively used as a standard probe for studying solvation dynamics.[33,34] Second, the ESIHT process in the hydrogen-bonded chelate ring of the *cis*-enol form has been predicted to play an important role in the efficient nonradiative deactivation process of the excited state.[12,14,16] Earlier studies on chemical systems having asymmetric intramolecular hydrogen-bonded chelate center and hence asymmetric potential energy surface (PES) for ESIPT reaction have established the fact that the ESIHT process is ultrafast and the lifetimes of these processes are in the range of a few hundred femtosecond (vide infra).[35–44] Since curcumin is a symmetric molecule with respect to the hydrogen-bonded chelate center (structures III and IV), it is unlikely that the ESIHT process leads to any change in the absorption and emission properties of the excited state to enable monitoring the process spectroscopically.

Recently, Adhikary et al. studied the excited-state photophysics of curcumin both in alcoholic solutions and in surfactant micelles using subpicosoecond fluorescence upconversion spectroscopy.[16,17] They reported the presence of two decay components in the excited-state kinetics with the lifetimes of about 12−20 and 100 ps in methanol and ethylene glycol (EG). The lifetime of the shorter component was nearly insensitive to deuteration, and this process was assigned to the process of solvation of the S_1 state. However, the lifetime of the longer component was seen to become longer due to deuteration and they assigned this component to the ESIHT process. When these papers were published, our group was engaged in investigating the dynamics of the excited states of curcumin using subpicosecond time-resolved transient absorption spectroscopic technique. However, the inferences from our studies were not exactly in conformity with those reported by Adhikary et al. and hence we intended to perform the fluorescence upconversion experiments to complement our inferences from the transient absorption experiments. In this paper, we report the results of our investigations on the relaxation dynamics of the excited states of curcumin in wide varieties of solvents, which include apolar aprotic, polar aprotic, and polar protic solvents, using both subpicosecond time-resolved fluorescence upconversion and transient absorption spectroscopic techniques.

2. Experimental Section

Curcumin obtained from Sigma Aldrich (purity ~80%) was purified by column chromatographic technique. Purity of the sample used here (better than 99%) was checked by HPLC.[12,13] Solvents were of spectroscopic grade (Spectrochem, Mumbai, India) and were used without further purification. Deuterated curcumin (curcumin-d_3, in which only the exchangeable hydrogen atoms of two phenolic groups and the enolic hydroxy group were replaced by deuterium atoms) was prepared by the following method: curcumin was dissolved in deuterated methanol (CH_3OD or methanol-*d*) solvent and kept in a dry nitrogen atmosphere for 24 h and then the solvent was evaporated. To ensure complete deuteration of the exchangeable hydrogen atoms, the process was repeated three times. Curcumin-d_3 was dissolved in methanol-*d* in nitrogen atmosphere for studying the effect of deuteration on the excited-state dynamics.

Steady-state absorption spectra were recorded on a Thermo-Electron model Biomate 5 spectrophotometer. Fluorescence spectra, which were corrected for the wavelength dependence of the instrument sensitivity, were recorded using Hitachi model 4010 spectrofluorometer. High-purity grade nitrogen gas (Indian Oxygen, purity >99.9%) was used to deaerate the samples, wherever required. All experiments were carried out at room temperature (298 K) unless specified otherwise.

The fluorescence upconversion spectrometer (FOG 100, CDP, Moscow) has been described in detail elsewhere.[45] In brief, laser pulses of 425 nm wavelength of 1 nJ energy/pulse and 100 fs duration are generated by frequency doubling the fundamental beam at 850 nm from a self-mode-locked Ti:sapphire oscillator (Tsunami, Spectra Physics) pumped by a 5 W DPSS laser (Millenia, Spectra Physics) using a 1 mm thick type I BBO crystal. These laser pulses were used to excite the sample in a 2 mm thick rotating quartz cell. The fluorescence photons emitted by the photoexcited sample are upconverted in a nonlinear BBO crystal of 0.5 mm thickness by mixing with the gate pulses, which consist of a portion of the fundamental beam. The upconverted light is dispersed in a monochromator and detected using photon counting electronics. A cross-correlation

function obtained using the Raman scattering from ethanol has a fwhm of 300 fs. The femtosecond fluorescence decays are fitted using a Gaussian function of the same fwhm for the instrument response function.

The time-resolved transient absorption spectra were recorded with subpicosecond time resolution (~100 fs) using a femtosecond pump−probe spectrometer. It uses a Ti:sapphire laser system, supplied by Thales Optronique SA, Elancourt, France, which provides the pulses of about 40 fs and 1 mJ energy per pulse at a repetition rate of 1 kHz. Pump pulses of 400 nm were generated for excitation of the samples by frequency-doubling of one part (150 μJ) of the 800 nm output of the amplifier in a 0.5 mm thick BBO crystal and the other part of the amplifier output was used to generate the white light continuum (470−1000 nm) probe in a 2 mm thick sapphire plate. The direction of polarization of the pump beam was fixed at the magic angle with respect to that of the probe beam and the energy of the pump beam was maintained at <5 μJ/pulse. The sample solutions were kept flowing through a quartz cell of 1 mm path length. To record the temporal profiles, wavelength regions of 10 nm width were selected using pairs of interference filters. The overall time resolution of the absorption spectrometer was determined to be about 120 fs. The temporal profiles recorded using different probe wavelengths were fitted with up to three exponentially decaying or growing components by iterative deconvolution method using a sech^2 type instrument response function with fwhm of 120 fs. To provide the lifetime values associated with each fit function, the notations "d" or "g" associated with the lifetimes, τ_1, τ_2, or τ_3, have been used for the component having a positive or negative exponent, to indicate whether the transient absorption signal is decaying or growing, respectively. Hence, the components representing the growth or decay of stimulated emission (SE) have been represented by the notation τ(d) or τ(g), respectively, in the insets of the figures. If the value of the lifetime is longer than 500 ps, this has not been indicated in the figures, since this value cannot be determined with reasonable accuracy by analyzing the temporal curve recorded up to 1.2 ns delay time.

3. Results

3.1. Steady-State Absorption and Fluorescence. Absorption and fluorescence spectra of curcumin have already been well characterized by different groups in different kinds of solvents and media.[12,14,15] However, for better understanding of the dynamics of the excited states in different kinds of solvents, we have compared and critically analyzed the characteristics of the absorption and fluorescence spectra of curcumin in four different kinds of solvents, namely, 1,4-dioxane (an aprotic solvent of low polarity), acetonitrile (a polar aprotic solvent), methanol (a polar protic solvent and a strong hydrogen bond donor), and dimethyl sulfoxide (DMSO) (a polar aprotic but a strong hydrogen bond acceptor) in Figure 1.[46] Curcumin has very low solubility in a nonpolar solvent, like cyclohexane (static dielectric constant, $\varepsilon_0 \sim 0$), and hence the subpicosecond dynamics of fluorescence or transient absorption could not be studied in this solvent. Therefore, we choose 1,4-dioxane ($\varepsilon_0 \sim 2.21$), which is a little more polar than cyclohexane, as the representative of the class of nonpolar aprotic solvents.

It is important to note that both the absorption and the fluorescence spectra exhibit significant solvent effect. Each of the absorption spectra presented in Figure 1 shows an intense absorption band in the 300−500 nm wavelength region. In 1,4-dioxane, acetonitrile, and methanol, the absorption maximum appears at the same wavelength (ca. 420 nm) with a shoulder

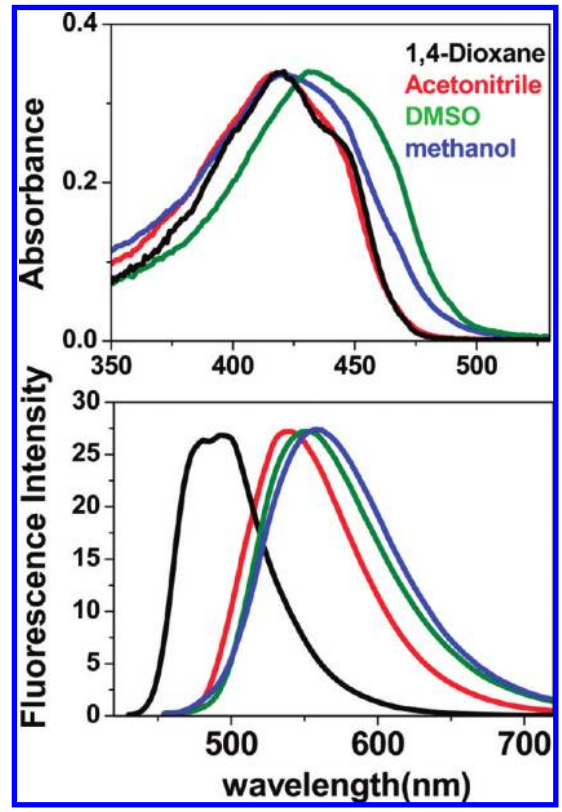

Figure 1. Steady-state absorption and fluorescence spectra of curcumin in 1,4-dioxane, acetonitrile, DMSO, and methanol.

at ca. 440 nm. However, in DMSO, the positions of both the absorption maximum and the shoulder are bathochromically shifted to 436 and 450 nm, respectively. It is also important to note that the intensity of the shoulder band increases significantly in methanol and DMSO, which are strong hydrogen bond donating and hydrogen bond accepting solvents, respectively. These facts suggest a significant perturbation of the intramolecular hydrogen bond existing in the *cis*-enol conformer and dictate the possibility of formation of intermolecular hydrogen-bonded complex in the ground state. However, formation of intermolecular hydrogen bond at the site of the phenolic OH groups too cannot be excluded.

Further, both the shapes and the wavelength maxima of the fluorescence spectra as well as the Stokes shifts are strongly dependent on the solvent characteristics. In 1,4-dioxane, the fluorescence spectrum shows a splitting of the maximum appearing at 480 and 494 nm. On the other hand, the same is broad with a maximum at 538 nm in acetonitrile, 550 nm in DMSO, and 560 nm in methanol. The Stokes shifts are about 3400, 5220, 4754, and 5950 cm^{-1} in 1,4-dioxane, acetonitrile, DMSO, and methanol, respectively. These values can be compared with that of about 1500 cm^{-1} in cyclohexane.[12] Larger Stokes shifts in more polar solvents is obviously a consequence of solvation because of a large change in dipole moment, $\Delta\mu$ (~6.1 D) following photoexcitation of curcumin to the S_1 state.[12] This implies that in the S_1 state, a reasonable amount of charge is transferred from the aromatic 4-hydroxy-3-methoxyphenyl moiety to the dicarbonyl moiety through π-conjugation.[27] As a consequence of this, the properties of the S_1 state are expected to have strong solvent dependence and solvation dynamics is likely to play an important role in the relaxation dynamics of the S_1 state of curcumin. However, the larger solvatochromic red shift observed in hydrogen bond donating solvent (methanol) can only be explained by the effect of both polarity and

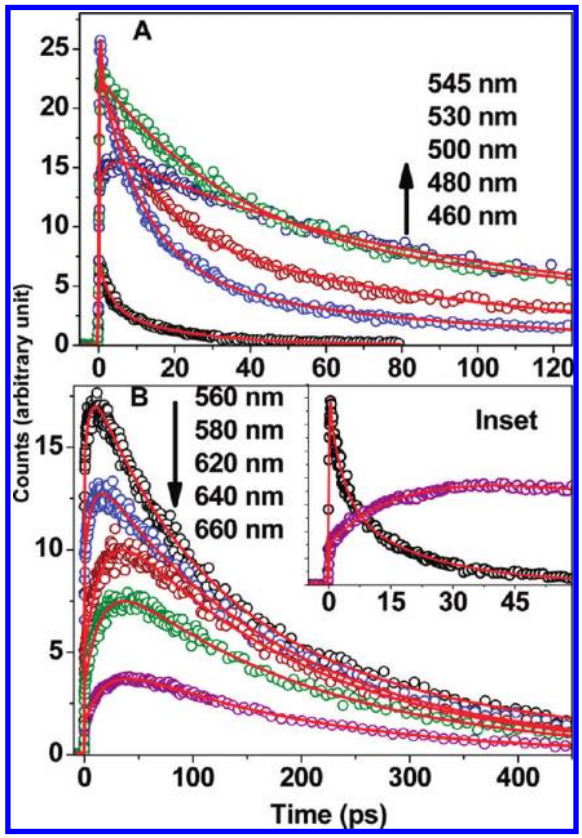

Figure 2. Fluorescence upconversion signals, recorded at different wavelengths, along with their biexponential or triexponential fit functions. Values of the lifetimes are given in Table 1. Inset of B: signals recorded at 460 and 660 nm have been compared in the sub-60 ps time domain to show the nearly equal rate of decay of the signal recorded at 460 nm and the rate of growth of the signal recorded at 660 nm.

hydrogen-bonding ability of the solvent on the excited state of curcumin. In our earlier work, we observed better linear correlation of the Stokes shift with the solvent polarity parameter, $E_T(30)$, as compared to that with the reaction field factor, ΔF.[12] This fact supported the prediction about strong hydrogen-bonding interaction between the S_1 state of curcumin and the solvents.

3.2. Fluorescence Upconversion Study. Figure 2 shows the fluorescence upconversion signals of curcumin in ethanol recorded in the 460−660 nm region using laser pulses of 425 nm of 100 fs duration. They have been analyzed by deconvolution of the effects of the finite temporal resolution of the fluorescence upconversion apparatus (fwhm of the instrument response function ~300 fs) from the measured emission decays. The fluorescence dynamics is nonexponential and shows significant wavelength dependence. The upconversion signals recorded in the 460−500 nm region could be well fitted using a triexponential decay function, whereas those recorded in the 515−660 nm region could be fitted using an exponential function consisting of an ultrafast growth component and another two decay components. In the 600−650 nm region, the inclusion of the decay component with a lifetime longer than 500 ps, but of very small amplitude, was essential to obtain a good fit. The best-fit function corresponding to each of the temporal curves has been shown in Figure 2, and the values of the different decay parameters associated with each of them have been given in Table 1. While the decay component with the lifetime of 200 ± 15 ps is associated with each of the upconversion signals presented in the Figure 2 region, the lifetimes of the other components, both the growth and the decay, are wavelength dependent. The presence of the long-lived component with the lifetime longer than 500 ps has already been reported in the fluorescence decay measured using the single photon counting technique and has been attributed to the presence of a small amount of other conformers, namely, the *trans*-diketo form, in the ground state (vide infra).[12,14,15]

This kind of fluorescence dynamics is the well-known characteristics associated with those chemical systems, such as coumarin 153, in which solvation plays a major role in the relaxation dynamics of the excited state of a molecule, which is created with a large molecular dipole moment following photoexcitation.[33,47,48] This information, in combination with the fact that the fluorescence spectra of curcumin exhibit larger Stokes shifts in more polar solvents, suggests that wavelength dependent dynamics observed in the fluorescence upconversion experiment is obviously a consequence of the solvation process. To delineate this aspect, we constructed the time-resolved emission spectra for the excited state of curcumin in ethanol at different delay times in the range 0.35−80 ps using the fluorescence upconversion signals collected at different wavelengths (Figure 2) using the method of Maroncelli and coworkers.[47] In brief, the deconvoluted multiexponential decay function at each monitoring wavelength is normalized so that its time integrated value matches with the emission intensity at the corresponding wavelength in the steady-state emission spectrum in the same solvent. This means that we assume that the emission spectrum of the "fully solvated" state recorded at infinite delay time corresponds to the steady-state emission spectrum in the same solvent. In this way, the normalized fluorescence intensity is known at all delay times in the 0.35−80 ps time domain for the entire set of monitoring wavelengths in the 460−660 nm region and the time-resolved emission spectra at different delay times are constructed by point-to-point plot of the emission intensities at different wavelengths. They have been presented in Figure 3.

The dynamic bathochromic shift of the emission maximum with an increase in delay time is the clear signature of the process of solvation of the excited state. However, a significant decrease in intensity of emission with increase in delay time is an indication of concomitant decay of the excited state during the solvation process. This suggests that association of the excited state of curcumin with the solvent molecules via intermolecular hydrogen-bonding induces faster nonradiative decay of the former. The frequency at which the maximum intensity appears in the time-resolved emission spectrum, shifts from 19 509 cm^{-1} recorded at 0.35 ps to 18 150 cm^{-1} recorded at 80 ps and hence the observed dynamic shift of the frequency maximum of the emission spectra due to solvation is about 1319 cm^{-1}.

It is a normal practice to construct the solvent correlation function, $C(t)$, as defined by eq 1, to determine the time constants associated with the solvation process.[33,47]

$$C(t) = \frac{\nu(t) - \nu(\infty)}{\nu(0) - \nu(\infty)} \quad (1)$$

Here, $\nu(0)$, $\nu(t)$, and $\nu(\infty)$, are the frequencies of the emission maxima at the delay times of zero (i.e., immediately after photoexcitation), intermediate time t, and infinity (i.e., after completion of the solvation process), respectively. To determine these emission maxima, we have used the peak frequency obtained directly from the log-normal fits of the corresponding spectrum. If we compare the position of the emission maximum

TABLE 1: Decay Parameters Obtained by Fitting the Fluorescence Upconversion Signals Presented in Figure 2, with the Multiexponential Function $f(t) = a_1 \exp(-t/\tau_1) + a_2 \exp(-t/\tau_2) + a_3 \exp(-t/\tau_3)$[a]

	decay parameters					
wavelength (nm)	τ_1, ps	a_1	τ_2, ps	a_2	τ_3, ps	a_3
460	1.8	0.43	13.9	0.52	200	0.05
480	1.95	0.15	13.6	0.68	195	0.17
500	3.7	0.15	23.9	0.6	180	0.25
515	0.07	−0.01	27	0.6	201	0.4
530	0.4	−0.04	30.5	0.55	199	0.45
545	5.9	−0.17	51.8	0.46	215	0.54
560	6.0	−0.27	52	0.32	210	0.68
580	6.2	−0.34	70	0.12	212	0.88
600	12.3	−0.49	190	0.92	long	0.08
620	16.2	−0.62	190	0.93	long	0.07
640	17	−0.66	195	0.92	long	0.08
660	19	−0.69	185	0.92	long	0.08

[a] All parameters reported in this table have a relative error of about 10−12%.

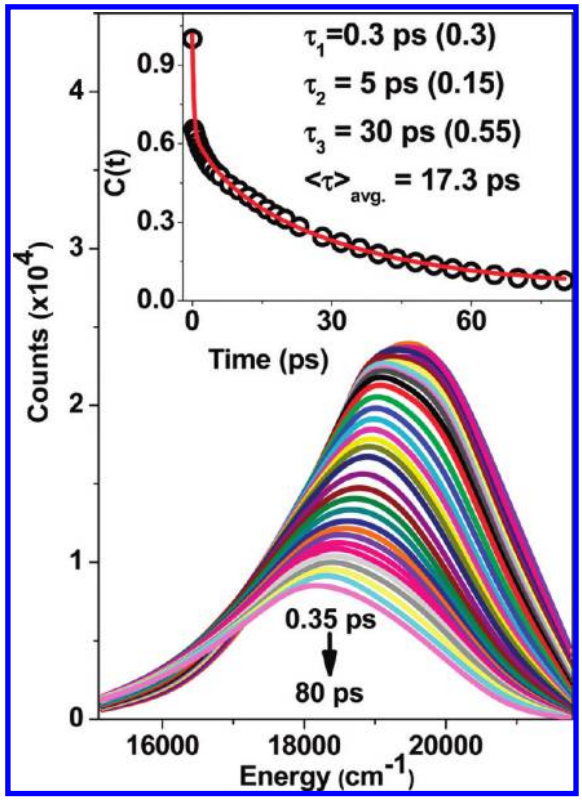

Figure 3. Time-resolved emission spectra constructed at different delay times (delay times: 0.35, 0.5, 0.8, 1.2, 1.6, 2.0, 2.5, 3, 3.5, 4.0, 5, 6, 8, 10, 12, 14, 16, 18, 20, 24, 28, 32, 36, 40, 44, 48, 52, 56, 60, 65, 70, 75, 80 ps). Inset: time-correlation function $C(t)$, constructed following eq 1, along with the triexponential fit function. The lifetimes associated with the fit function and the average lifetime calculated are also shown in the inset.

of the spectrum, which could be recorded at the earliest delay time, i.e., 19 509 cm^{-1} at 0.35 ps, with that of the fluorescence spectrum recorded in a nonpolar sovent, i.e., at about 20 000 cm^{-1} in cyclohexane,[12] it becomes evident that we have missed the early events of solvation phenomena, which have been completed prior to the delay time of 0.35 ps. So, because of limitation of the instrument response of about 300 fs, we have not been able to record the emission spectrum of the unsolvated species, which exists only at zero delay time. Hence, the value of $\nu(0)$ could not be determined in this experiment. However, accepting the value of 20 000 cm^{-1} as that of $\nu(0)$ should be a good approximation. The maximum of the emission spectrum recorded at the delay time of 80 ps is seen to appear at 18 150 cm^{-1}. This corresponds to that for the steady-state fluorescence spectrum recorded in ethanol and this is the assumption made for construction of the time-resolved fluorescence spectra presented in Figure 3. This value is assigned to $\nu(\infty)$. Thus the correlation function, $C(t)$, constructed using eq 1 has been shown in the inset of Figure 3. This curve also includes the point for which the value of $C(t)$ is equal to 1. The $C(t)$ curve could be fitted using a triple exponential function, which provides the lifetimes of the components with their relative amplitudes as 0.3 ps (0.3), 5 ps (0.15), and 30 ps (0.55). The average solvation time could be calculated as 17.3 ps and it agrees well with the value determined in ethanol using standard solvation probes ($\langle\tau\rangle_{avg} \sim 16$ ps).[47,48]

In Figure 4, we have compared the fluorescence upconversion signals for curcumin in methanol and curcumin-d_3 in methanol-d recorded at a few selective wavelengths, namely 480, 520, and 640 nm. While in all the cases, the fluorescence upconversion signals are fitted with multiexponential functions consisting of decay and/or growth components, the lifetimes of each of the corresponding components is longer in the case of deuterated solute and solvent. However, the effect of deuteration is seen to be more prominent at the longer monitoring wavelengths and at longer delay time. This information, in combination with that obtained from the fluorescence upconversion experiment performed in ethanol (Figures 2 and 3), confirms the fact that association of the excited state of curcumin with the solvent molecules becomes stronger as the solvation process proceeds to completion and it involves the formation of intermolecular hydrogen (or deuterium, in the case of deuterated solute and solvent) bonds between the solute and the solvent, which is accompanied by reorganization of the hydrogen (or deuterium) bonds of the solvent around the solute molecule (vide infra). Stretching vibrations in hydrogen (or deuterium) bonds induce fast nonradiative deactivation of the excited state, and hence the longer lifetimes of the corresponding components in the case of curcumin-d_3 in methanol-d as compared to those of curcumin in methanol are the result of the deuterium isotope effect, imparted to strong intermolecular hydrogen-bonding interaction between the S_1 state of curcumin and the solvent.

Adhikary et al. reported the lifetimes of the S_1 state of curcumin as 70 and 120 ps in methanol and methanol-d_4, respectively, on the basis of their measurement at 520 nm.[16] However, our results described above show that the fluorescence decay monitored at this wavelength cannot provide the correct value of the lifetime of the fully relaxed or solvated S_1 state. Because of the dynamic shift of the fluorescence maximum

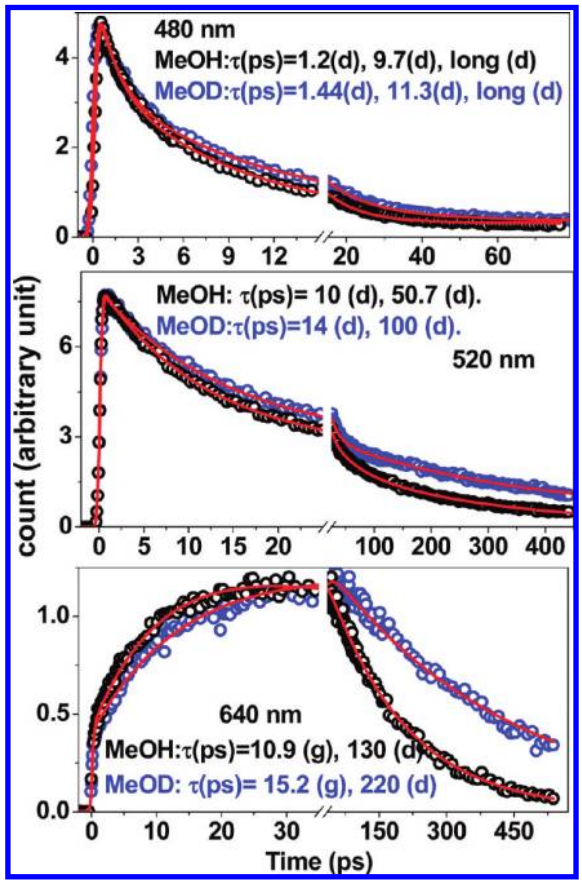

Figure 4. Comparison of the flurescence decay of curcumin in methanol and curcumin-*d* in methanol-*d* at 480, 520, and 640 nm.

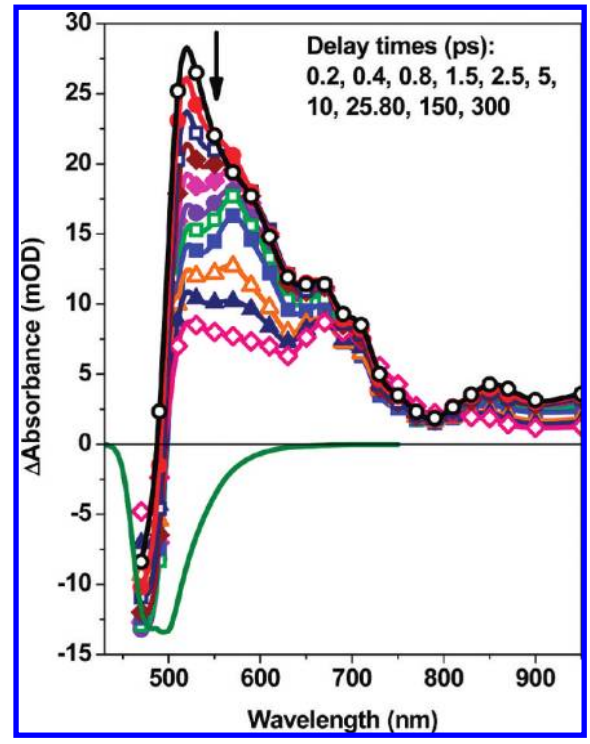

Figure 5. Time-resolved differential absorption spectra of the transient species formed after photoexcitation of curcumin in 1,4-dioxane using the 400 nm laser. The green curve represents the position and shape of the steady-state fluorescence spectrum.

representing the progress of solvation phenomenon, the fluorescence decay monitored at different wavelengths through the entire region of the fluorescence spectrum is wavelength dependent and nonexponential. Hence, the analyses of the upconversion signals recorded in the 460−600 nm region cannot provide any meaningful information about either the solvation time or the lifetime of the S_1 state. Since, at these wavelengths, we monitor a nonequilibrium mixture of differently solvated excited-state species, the lifetimes obtained by multiexponential fitting of the fluorescence decay represents the average values of the lifetimes of a large number of differently solvated species. Meaningful information can be obtained by monitoring the fluorescence decay only at the red edge of the fluorescence spectrum, e.g., at 640−660 nm, at which the fully solvated S_1 state can be monitored. At 640 or 660 nm, the growth of the upconversion signal represents the formation of the fully solvated species and the decay lifetime of the signal can be assigned to that of the solvated species. Therefore, we find that the decay lifetimes of the S_1 state of curcumin in methanol and curcumin-d_3 in methanol-*d* are 130 ± 7 and 220 ± 10 ps, respectively. These lifetimes are longer than those reported by Adhikary et al. because of the reason explained above. Further, we have shown in the case of curcumin in ethanol that the solvation in alcoholic solvents is multimodal and hence the single exponential growth of the S_1 state monitored at 640 nm (or at any other wavelength) cannot provide the complete information regarding the solvation dynamics. However, the growth lifetimes, 10 ± 1 or 14 ± 1 ps, measured at this wavelength can be described as the longest component of the multimodal solvation process of curcumin in methanol or curcumin-d_3 in methanol-*d*, respectively (see section 4.1).

3.3. Transient Absorption Spectroscopic Study. ***3.3.1. In Aprotic Solvents.*** Fluorescence upconversion experiments revealed that intermolecular hydrogen-bonding interaction via hydrogen bond reorganization is possibly the major process contributing to the relaxation of the S_1 state of curcumin in alcoholic solvents. However, this technique has not revealed the role of any other process, such as photoisomerization via twisting of the double bonds. In addition, the dynamics of the S_1 state of curcumin in aprotic solvents has not been studied earlier, and hence the aspect of solvation of curcumin in this class of solvents is yet unexplored. These are the reasons, which motivated us to investigate the relaxation dynamics of the S_1 state of curcumin in different kinds of solvents using the transient absorption spectroscopic technique, which has a better time resolution (∼100 fs) then the fluorescence upconversion method.

Figure 5 presents the time-resolved differential absorption spectra of the transient species created following photoexcitation of curcumin in 1,4-dioxane using 400 nm laser pulses of about 50 fs duration. The transient spectrum recorded at 0.2 ps delay time consists of one negative absorption band in the 470−500 nm region (the entire band could not be recorded here because of limitation of the spectrometer) and a broad positive absorption band due to excited-state absorption (ESA) in the 500−830 nm region. A comparison between the steady-state spectra (both absorption and fluorescence) of curcumin in 1,4-dioxane (Figure 1) and the negative absorption band observed here yeilds the latter could obviously be assigned to stimulated emission (SE) and not to bleaching. In addition, comparison of the shapes and positions of the steady-state fluorescence spectrum and the transient spectra, as shown in Figure 5, suggests the overlap of the SE and ESA bands in the 450−550 nm region. With increase in delay time, both the SE and ESA bands decay. However, the pattern of evolution of the time-resolved spectra suggest that the decay of the ESA band in the lower energy (e.g., in the

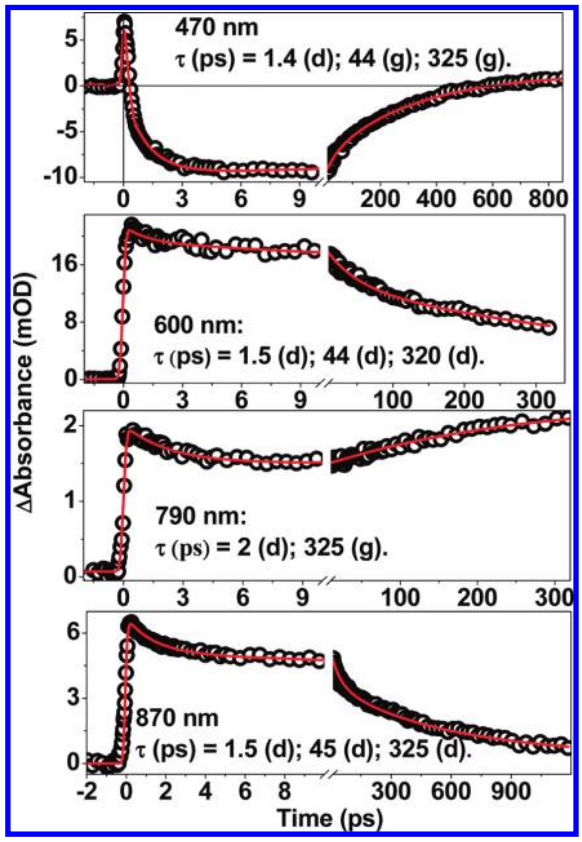

Figure 6. Temporal profiles (circles) recorded at a few selective wavelengths following photoexcitation of curcumin in 1,4-dioxane using 400 nm light. The red lines represent the best fit multiexponential functions, and the lifetimes associated with the best fit function are given in the insets.

650−700 nm) region is slower than that in the higher energy (e.g., in the 500−650 nm) region. Further, in the 700−770 nm region, we observe an ultrafast decay of transient absorption followed by a growth (see Figure 6). All these characteristics lead to wavelength-dependent temporal dynamics (see Figure SM1 in the Supporting Information), which suggest the involvement of more than one transient species or excited states in the relaxation dynamics of curcumin in this solvent.

In Figure 6, we have presented the temporal profiles recorded at a few selective wavelengths following photoexcitation of curcumin in 1,4-dioxane. The best-fit functions are also presented in this figure along with the lifetimes associated with the different components in the insets. Temporal profiles recorded in the 500−600 nm region show wavelength dependent dynamics because of overlapping of SE and ESA bands in this region. However, those recorded in the 470−500 nm region and in the 600−1000 nm region are expected to provide useful information regarding the dynamics of the S_1 state. The temporal profiles presented in Figure 6 could be best fitted by a four exponential (those recorded at 470, 590, and 870 nm) or three exponential (that at 790 nm) function consisting of both decay and growth components and the lifetimes of the components associated with these temporal profiles are seen to be very similar. This suggests that at least three excited states or processes are responsible for the evolution of the transient spectra presented in Figure 5. Nardo et al. also have found that in cyclohexane, a nonpolar aprotic solvent like 1,4-dioxane, the fluorescence decay of curcumin is triexponential (with the lifetimes of 57, 256, and 1405 ps).[14] Unfortunately, spectral characteristics of these four kinds of transient species could not be resolved in the transient spectra because of overlapping of the ESA and SE bands throughout the wavelength region. The average lifetimes of three of these processes could be determined as 1.6, 44, and 325 ps. Another component has a lifetime longer than 500 ps. Each of the temporal profiles recorded at different wavelengths in this solvent (and in any other solvent studied here) is associated with a long-lived component, which has a lifetime longer than 500 ps. Since we have not been able to determine this value with sufficient accuracy (because of limited length (25 cm) of our linear translational stage used for the delay line), it has not been shown in the insets of the figures.

It should be noted that the lifetimes of the two shorter lived components (44 and 325 ps) determined by us in 1,4-dioxane are comparable to those determined in cyclohexane (57 and 256 ps, respectively) by Nardo et al.[14] In the present work, we could not determine the lifetime of the longest component with reasonable accuracy, which has the contribution of only about a few percent. The presence of a long-lived decay component with the lifetime of about 1100 ps, in addition to the shorter lived component with 52 ps lifetime, in the fluorescence decay in benzene has also been reported by Khopde et al.[12] In the present case, however, the long-lived decay component of transient absorption may have contribution from the decay of the triplet state, which has the lifetime of a few microseconds, and hence, we will not discuss here about the origin of this component having lifetime longer than 500 ps.[12,14]

Comparison between the relative amplitudes associated with the components having the lifetimes of 57 ps (83%) and 256 ps (16%) in cyclohexane and the relative abundance of the *cis*-enol and *trans*-diketo conformers (about >95% and <5% respectively) of curcumin in the ground state have led Nardo et al. to assign these two lifetime components to these conformers (see section 1).[12,14,21−25] Following the same arguments, we too assign the components with the lifetimes of 44 and 325 ps determined in 1,4-dioxane to the S_1 states of the *cis*-enol and *trans*-diketo conformers, respectively. We find that this assignment is quite justified since both the *cis*-enol and *trans*-diekto isomers absorb 400 nm light to be excited to the S_1 state. However, the lifetime of the *trans*-diketo isomer is expected to be longer because of the absence of the nonradiatve decay via hydrogen stretching vibrations unlike in the case of the *cis*-enol form.

Further, since the component with the lifetime of 1.6 ps is quite in agreement with the value of the average solvation time, $\langle\tau\rangle_{coum}$ (~1.7 ps), determined using coumarin 153 as a probe for solvation dynamics in the same solvent (Table 2), it possibly can be assigned to the solvation process.[47] However, we need to discuss the results in other solvents to confirm the assignment of this ultrafast component.

We have also recorded the temporal profiles at 470 and 870 nm following photoexcitation of curcumin in ethyl acetate (EA) and glycerol triacetate (or triacetin, TA). They, along with the best-fit functions and the associated lifetimes, have been presented in Figure SM2 in the Supporting Information. These are moderately polar aprotic solvents, but TA is highly viscous (see Table 2). Similar results, as those obtained in the case of 1,4-dioxane, were obtained in these solvents and the values of the lifetimes are presented in Table 2. However, in these cases, we find an additional ultrafast component, which could be assigned to the intramolecular vibrational relaxation (IVR) process in the S_1 state (vide infra).[49−51]

Figure 7 presents the time-resolved differential absorption spectra of the transient species generated following photoexcitation of curcumin in acetonitrile, which can be considered as a polar aprotic solvent. The transient absorption spectrum

TABLE 2: Lifetimes of the Processes Associated with the Relaxation Dynamics of the Excited States of Curcumin in Different Kinds of Solvents, Determined Using the Transient Absorption Spectroscopic Technique[a]

solvent	ε_0,[b] η (cP)[c]; β-,[c]; E_T^N [c]	τ_I, τ_{II}, τ_{III}, ps[d]	τ_L, ps[e]; $\langle\tau\rangle_{coum}$, ps[f]	τ_v, ps[g]	solvation components			τ_3, ps
					τ_1, ps (a_1)	τ_2, ps (a_2)	$\langle\tau\rangle_{solv}$ ps	
1,4-dioxane	2.2; 1.42; 0.37; 0.164	2.2, 18.3, −	−; 1.7			1.6 ± 0.2	1.6 ± 0.2	44 ± 3
EA	6.0; 0.43; 0.45; 0.228	0.21, 1.7, −	1.6; 2	0.5 ± 0.1		6 ± 0.5	6 ± 0.5	230 ± 10
TA	7.3; 20; −; 0.34	−, −, −	−; 49.5	1.4 ± 0.2		50 ± 5	50 ± 5	300 ± 15
BN	25.2; 1.24; −; 0.833	0.36, 5.3, 25	12.5; 5.1	0.3 ± 0.1	6.7 ± 0.5 (0.37 ± 0.05)	21 ± 3 (0.63 ± 0.05)	15.7 ± 1	270 ± 10
acetonitrile	35.8; 0.34; 0; 0.46	0.09, 0.63, −	0.2; 0.5		0.3 ± 0.05 (0.61 ± 0.05)	0.65 ± 0.1 (0.39 ± 0.04)	0.44 ± 0.02	300 ± 15
DMF	36.7; 0.8; 0.69; 0.722	0.22, 1.7, 29.1	2.1; 0.92		0.3 ± 0.05 (0.36 ± 0.03)	2.9 ± 0.5 (0.64 ± 0.05)	1.6 ± 0.3	155 ± 10
DMSO	46.5; 1.99; 0.76; 0.444	0.21, 2.3, 10.7	2.1; 1.8		0.4 ± 0.05 (043 ± 0.04)	3.3 ± 0.5 (0.57 ± 0.05)	1.8 ± 0.3	175 ± 10
PC	64.9; 13; 0.4; 0.491	0.18, 2.03, 6.57	8; 2.6		1 ± 0.2 (0.39 ± 0.03)	6.3 ± 0.5 (0.63 ± 0.05)	4.4 ± 0.8	285 ± 15
formamide	111; 3.3; 0.55; 0.799	0.16, 2.9, 57.9	−; 5.0		0.34 ± 0.1 (0.5 ± 0.03)	3.5 ± 0.3 (0.5 ± 0.03)	1.1 ± 0.3	45 ± 5
methanol	32.7; 0.55; 0.62; 0.762	0.28, 3.2, 15.3	9.2; 5	0.2 ± 0.1	1.5 ± 0.2 (0.37 ± 0.03)	10 ± 1 (0.63 ± 0.05)	6.9 ± 0.8	130 ± 10
ethanol	24.6; 1.08; 0.77; 0.654	0.39, 5.0, 29.6	28.1; 16		3 ± 0.5 (0.25 ± 0.02)	27 ± 2 (0.75 ± 0.05)	21 ± 2	290 ± 15
1-propanol	20.5; 1.94; −; 0.617	0.34, 6.6, 47.8	58.7; 26		4 ± 1 (0.11 ± 0.01)	40 ± 3 (0.89 ± 0.06)	36 ± 3	410 ± 15
1-butanol	17.5; 2.57; −; 0.602	5.03, 42.6, 133	100; 63		17 ± 2 (0.17 ± 0.01)	77 ± 5 (0.83 ± 0.06)	67 ± 5	630 ± 20
1-pentanol	13.9; 3.51; −; 0.568	0.67, 21.7, 151	152; 103		30 ± 3 (0.2 ± 0.01)	155 ± 10 (0.8 ± 0.6)	130 ± 6	1150 ± 50
EG	37.7; 13.8; −; 0.790	5, 32	86; 15		2 ± 0.5 (0.47 ± 0.04)	18 ± 3 (0.53 ± 0.05)	10.5 ± 2	231 ± 10

[a] Only the lifetimes shorter than 500 ps have been given here. [b] ε_0 is the static dielectric constant.[47] [c] η is the viscosity, and β and E_T^N are values of the solvents.[46] [d] (τ_I, τ_{II}, τ_{III}) are the lifetimes associated with the multimodal solvation determined using C153 probe.[47] [e] Longitudinal relaxation times.[48,52] [f] The average solvation time, $\langle\tau\rangle_{coum}$, determined using Coumarin153 probe.[47,48] [g] Vibrational relaxation time (see text). [h] This lifetime is assigned to the *trans*-diketo conformer, which has lifetime longer than 500 ps in other solvents.

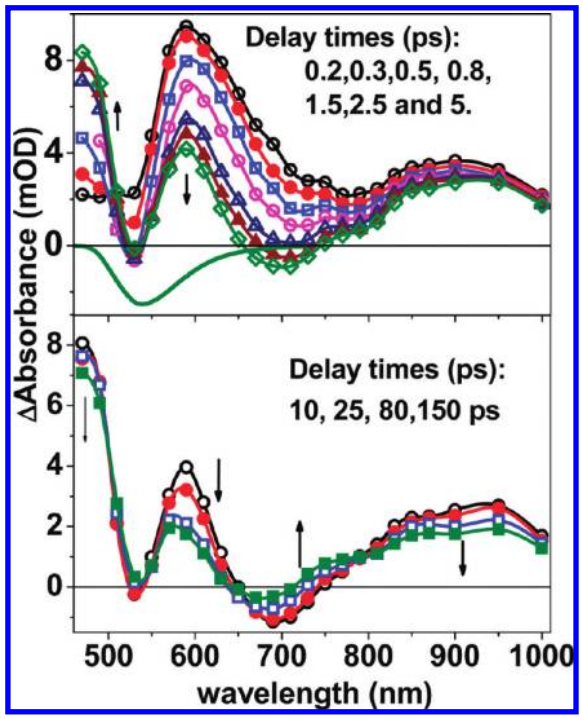

Figure 7. Time-resolved absorption spectra of the transient species formed following photoexcitation of curcumin in acetonitrile using 400 nm laser pulses.

recorded at 0.2 ps delay time shows the presence of two broad ESA bands with maxima at ca. 590 and 900 nm. We do not observe an SE band in the 500−700 nm region, where the fluorescence emission band of curcumin in acetonitrile occurs (Figure 1), but a small negative absorption at 530 nm. The observed differential transient spectrum is the result of additive combination of SE and ESA bands in this wavelength region. With an increase in the delay time in the sub-5 ps time domain, we observe the decay of the ESA band in the 550−800 nm region with the concomitant development of an ESA band in the 470−500 nm region. This evolution also leads to the development of a weak SE band with a maximum at ca. 700 nm. It is also important to note that decay of the ESA band in the 530−800 nm region is faster than that in the 800−1000 nm region, which does not show any significant change in this time domain. Evolution of the time-resolved spectra looks apparently different from that observed in 1,4-dioxane, because of the fact that the fluorescence spectrum is shifted significantly toward the lower energy region as compared to that in the case of 1,4-dioxane, leading to the overlap of ESA and SE bands in a spectral region, which is different from that in the case of 1,4-dioxane. However, analyses of the temporal profiles reveal the involvement of similar kinds of processes in the relaxation of the excited states of curcumin in these two solvents as well as in other solvents discussed earlier.

The pattern of evolution of the time-resolved transient absorption spectra in acetonitrile also supports these facts. Development of the ESA band in the 470−500 nm region and the SE band in the 650−750 nm region with an increase in delay time is the result of the dynamic bathochromic shift of the SE band but hypsochromic shift of the ESA band due to solvation of the excited state. That is why the shapes of the temporal profiles recorded in the 500−700 nm region and the corresponding lifetimes of the different components are wavelength dependent (see Figure SM3 in the Supporting Information). Since, the steady-state fluorescence spectrum of curcumin in acetonitrile has very weak intensity in the 470−490 nm region (Figure 1), the ESA band is expected to be free from interference from the SE band in this region. Therefore, the temporal profiles recorded in this region are expected to provide meaningful results regarding the lifetimes of the excited states or the processes associated with them. On the basis of similar arguments, temporal profiles recorded in the 700−1000 nm region are also expected to provide meaningful values of the lifetimes. At delay times longer than 5 ps, we observe the decay of all the ESA and SE bands occurring in the entire wavelength region, but a marginal increase of ESA in the 700−800 nm region.

In Figure 8, we have presented the temporal profiles recorded at a few selective wavelengths following photoexcitation of curcumin in acetonitrile. The temporal profiles recorded in the 470−490 nm region could be fitted with a four exponential function consisting of two ultrafast growth components of ESA with the lifetimes of 0.3 and 0.65 ps, followed by its two exponential decay with the lifetimes of 310 ps and a long-lived component having lifetime longer than 500 ps, which is not shown in the insets of the figure. However, those at other wavelengths could be fitted well with three exponential functions consisting of both decay and growth components. Although the ultrafast component with the lifetime of 0.3 ps is not evident in

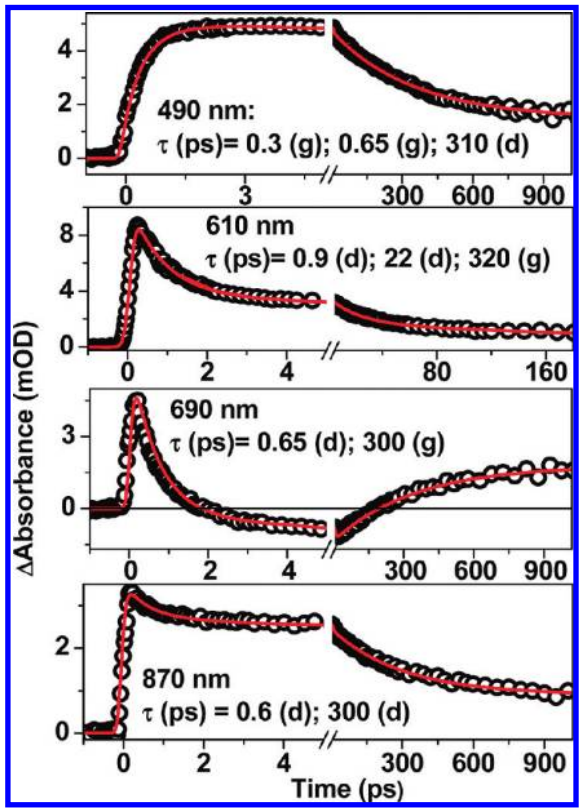

Figure 8. Temporal profiles (circles) recorded at a few selective wavelengths following photoexcitation of curcumin in acetonitrile. The red lines represent the best fit multiexponential functions. The lifetimes associated with the fit functions are given in the insets. In each case, the fit function is associated with a slow decay component with a lifetime longer than 500 ps, which is not given in the insets.

the temporal profiles recorded at wavelengths other than 470 nm, the values of the other two lifetimes determined at 690 and 870 nm are very similar to those determined at 470 nm. The values of two of the three lifetimes, determined at 610 nm, do not agree well with those determined at other wavelengths possibly because of overlapping of SE and ESA bands at this wavelength. Average values of the lifetimes of the three components determined at 490, 690, and 870 nm in acetonitrile are shown in Table 2.

Temporal profiles have been recorded at 470 and 870 nm in other polar aprotic solvents, namely, benzonitrile (BN), dimethylformamide (DMF), DMSO, propylene carbonate (PC), and formamide. While the temporal profiles recorded in BN are shown in Figure SM2 in the Supporting Information, those recorded in the other four solvents are shown in Figure 9. Temporal profile recorded at 470 nm in BN could only be fitted by a four exponential function with the components having lifetimes of 0.3 ps (d), 6.7 ps (g), 21 ps (g), and 400 ps (d). While that recorded at 870 nm has been fitted with a four exponential function with the lifetimes of 1 ps (d), 18 ps (d), 250 ps (d), and >500 ps (d). In the latter case, possibly two ultrafast components (0.3 and 6.7 ps) could not be resolved but an average value of 1 ps has been obtained. Temporal profiles recorded at 470 nm in each of the other four solvents have been well-fitted with an exponential function consisting of two growth components and two decay components. That recorded at 870 nm could be fitted well with a four exponential decay function. The lifetimes of three shorter lived components (but not the one with lifetime longer than 500 ps) associated with the multiexponential best-fit function are given in the caption of the figure. The lifetimes of the corresponding components are very similar at these two wavelengths in each of these solvents and the average values of these lifetimes determined from these two measurements are given in Table 2. It is important to note that viscosities of DMSO and PC are 6 and 40 times, respectively, larger than that of acetonitrile. Further, the polarity of formamide is more than about 3 times larger than that of acetonitrile.

3.3.1. In Protic Solvents. To delineate the aspect that solvation is the major process involved in the relaxation of the

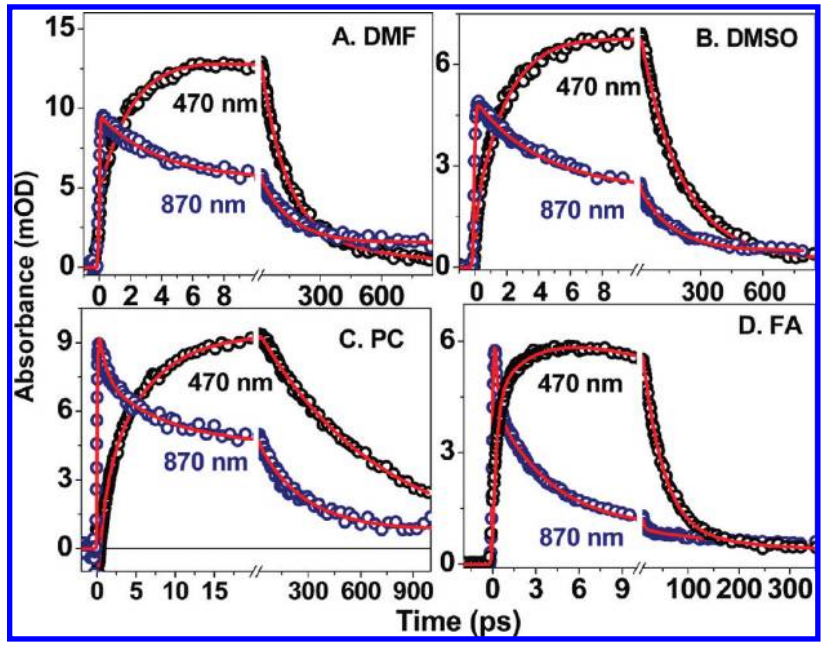

Figure 9. Temporal profiles (circles) recorded at 470 and 870 nm following photoexcitation of curcumin in polar aprotic solvents. The red lines represent the best fit multiexponential functions. The lifetimes (in ps) associated with the fit functions are as follows (in each case the fit function is associated with a slow decay component with a lifetime longer than 500 ps, which is not given here). (A) DMF: 470 nm 0.3 (g), 2.3 (g), 162 (d); 870 nm 3.5 (d), 150 (d). (B) DMSO: 470 nm 0.35 (g), 2.6 (g), 202 (d); 870 nm -4 (d), 160 (d). (C) PC: 470 nm 1 (g), 6.3 (g), 300 (d); 870 nm 1 (d), 7.7 (d), 270 (d). (d) FA: 470 nm 0.3 (g), 3.2 (g), 42 (d); 870 nm 0.25 (d), 3.9 (d), 50 (d).

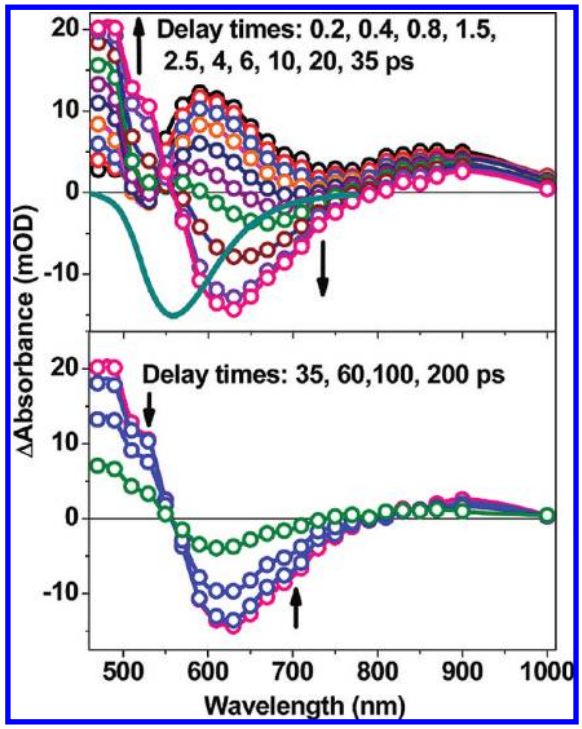

Figure 10. Time-resolved differential absorption spectra of the transient species formed following photoexcitation of curcumin in methanol. The green curve represents the steady-state fluorescence spectrum in this solvent.

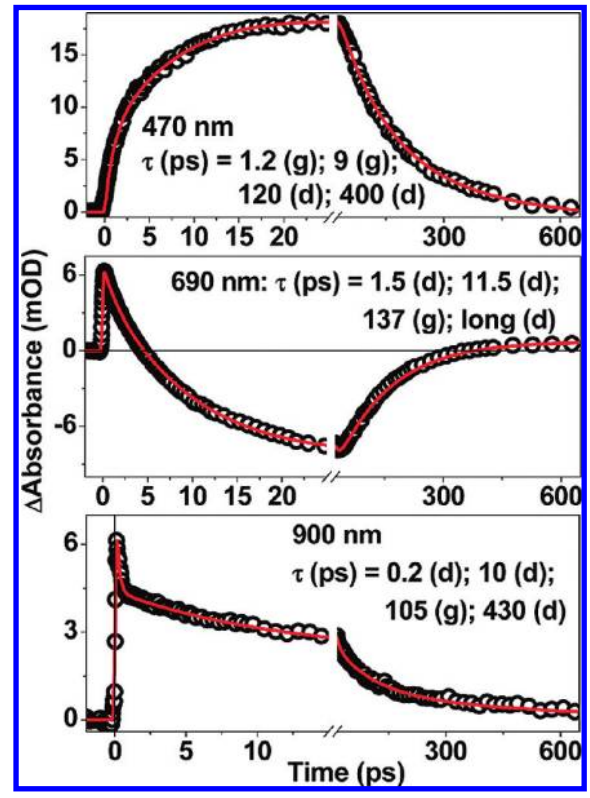

Figure 11. Temporal profiles (circles) recorded at a few selective wavelengths following photoexcitation of curcumin in methanol. The red lines represent the best fit multiexponential functions. The lifetimes associated with the fit functions are given in the insets.

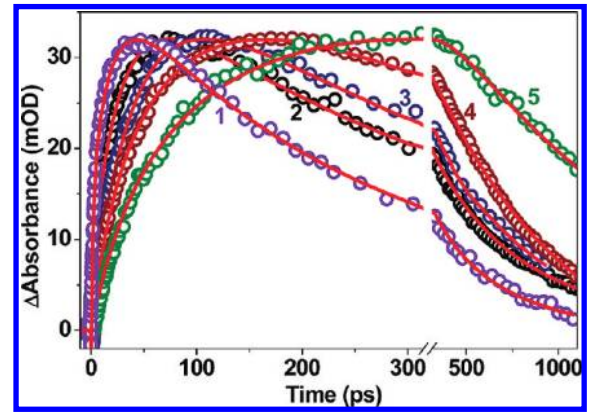

Figure 12. Temporal profiles recorded at 480 nm following photoexcitation of curcumin in alcohols: EG (1), ethanol (2), 1-propanol (3), 1-butanol (4), and 1-pentanol (5). Lifetimes obtained from the best fit multiexponential finction are given in Table 2.

excited state of curcumin in alcohols, as revealed by the transient fluorescence spectroscopic study, we investigated the properties of the excited states in the series of normal alcoholic solvents. Evolution of the transient absorption spectra of the transient species generated following photoexcitation of curcumin in methanol has been shown in Figure 10. Spectral characteristics of the transient species formed in this solvent are very similar to those observed in acetonitrile. As discussed in the case of acetonitrile, dynamic hypsochromic and bathochromic shifts of strongly overlapping ESA and SE bands, respectively, occurring in the 500−750 nm region are responsible for the evolution of the time-resolved spectra presented in this figure. However, in this case, we observe the reverse dynamic shift of the SE band, which is the net result of combination of the two opposite kinds of spectral shifts undergone by the ESA and SE bands. As a consequence of this, occurrence of wavelength dependent dynamics in the 500−700 nm region is obvious in this case too. Following the same arguments as presented earlier, the lifetimes of the components, which have lifetimes shorter than 500 ps, could be determined accurately by analyzing the temporal profiles recorded in the 470−490 and 700−1000 nm regions. In Figure 11, we have presented the temporal profiles recorded at a few selective wavelengths. As in aprotic solvents (except acetonitrile), analysis of the temporal profiles recorded in the 470−490 nm region reveals four exponential dynamics, which includes the contribution of a component with a lifetime of 400 ps (also shown in Table 2). In other solvents, this component is longer than 500 ps. However, in the case of the temporal profiles recorded in the 800−1000 nm region, inclusion of an ultrafast decay component with a lifetime of 0.25 ps has been found necessary to fit the ultrafast decay part, in addition to the four other decay components. The average values of the lifetimes determined from the measurements at these three wavelengths are given in Table 2.

Considering the better strength of the transient absorption signal at 480 nm and also the fact that accurate information about the lifetimes is available at this wavelength because of negligible overlap between the ESA and SE bands, temporal profiles have been recorded at this wavelength in other normal alcoholic solvents (i.e., ethanol to 1-pentanol) as well as in ethylene glycol (EG) (Figure 12). Each of the temporal profiles presented in this figure could be best fitted with a four exponential function consisting of two ultrafast growth components (τ_2 and τ_2) and two decay components (τ_3 and τ_4). While in methanol, τ_4 is about 425 ps, in other alcoholic solvents, it is longer than 500 ps and the same is not given in Table 2. It is important to note that for the alcoholic solvents used here, the viscosity varies from 0.55 in methanol to 3.51 in pentanol and 13.8 in EG and the average solvation time, $\langle\tau\rangle_{coum}$, varies from 5 ps in methanol to 103 in pentanol (Table 2). However, $\langle\tau\rangle_{coum}$ of EG (15.3 ps) is nearly equal to that of ethanol (∼16

ps), the viscosity of which ($\eta \sim 1.08$ cP) is much smaller than that of EG ($\eta \sim 13.8$ cP). The lifetimes of different components, which are presented in Table 2, show a large variation with the change in solvent characteristics. However, a preliminary observation reveals that while the τ_1 and τ_2 seem to have a better correlation with the solvation time rather than the viscosity, τ_3 may be better correlated with the hydrogen-bonding ability (measured by E_T^N values) in alcoholic solvents (vide infra).

4. Discussion

4.1. Solvation Dynamics. In the present study, we have combined two complementary ultrafast techniques, namely, subpicosecond fluorescence upcoversion and transient absorption spectroscopy to investigate the dynamics of the excited states of curcumin in different kinds of solvents. Our fluorescence upconversion study in ethanol (section 3.2) has established beyond doubt that the solvation process has a major contribution in the relaxation of the S_1 state of curcumin in alcohols. It has also been established that the solvation process is multimodal with three components having lifetimes of 0.3, 5, and 30 ps in ethanol and the average solvation time, $\langle\tau\rangle_{solv}$, could be calculated as 17.3 ps (Figure 3). To compare them with the values of τ_1 (=3 ps) and τ_2 (=27 ps) (Table 2) determined by us in ethanol using the transient absorption technique, we find that this technique provides an average value of 2 ps for two ultrafast components (0.3 and 5 ps), and the value of τ_2 (27 ps) agrees well with that (30 ps) of the longest component associated with the $C(t)$ function (eq 1), determined using the fluorescence upconversion technique. They also correspond well to the longitudinal relaxation time, ($\tau_L \sim 28.1$), of the solvent (Table 2). It is also important to note that the lifetimes of the three components associated with the $C(t)$ function are in good agreement with the lifetimes, τ_I, τ_{II}, and τ_{III} (Table 2) associated with the multiexponential fit of the spectral response function determined by Maroncelli and his co-workers using the standard solvation probe, coumarin 153.[35] The average solvation time, $\langle\tau\rangle_{solv} = 17.3$ ps) determined by us also agrees well with that (16 ps) reported by these authors. In addition, the value of τ_2 in methanol is in perfect agreement with the lifetime of the component of 10 ps lifetime determined by Adhikary et al., who also assigned this component to solvation process.[16] Therefore, these arguments establish that the two ultrafast components (namely, τ_1 and τ_2) associated with the relaxation dynamics of the S_1 state of curcumin in normal alcohols are associated with the solvent reorganization process and further confirm that in alcoholic solvents, solvation plays a major role in it.

We discussed earlier that curcumin adopts mainly the intramolecular hydrogen-bonded *cis*-enol form (Scheme 1), with minor amounts of the *trans*-diketo conformer, which has a much smaller dipole moment (1.41 D) than that of the former (~10.8 D).[21] However, in polar hydrogen-bonding solvents, the intramolecular hydrogen bond is perturbed significantly because of formation of an intermolecular hydrogen bond. Increased absorption in the lower energy region of the absorption spectrum as well as large Stokes shifts in both polar and hydrogen-bonding solvents suggest that both polarity and intermolecular hydrogen bonding perturb the intramolecular hydrogen bond existing in the *cis*-enol conformer.[12,14] Therefore, the results presented in this work regarding the dynamics of the excited states of curcumin in alcoholic solvents describe the dynamics of *specific interaction* between the solute's electronic state and the solvent via intermolecular hydrogen bonding, which is accompanied by the reorganization of the hydrogen-bonding network structure of the alcoholic solvent. Berg and co-workers established the fact that solvent dynamics affecting the hydrogen bond reorganization time of the solvent is well correlated with the dielectric relaxation time or the longitudinal dielectric relaxation time, τ_L.[54,55] Several groups of workers reported nonexponential solvation dynamics in *n*-alcohols.[47,48,52,56–58] The short component observed in *n*-alcohols is shorter than τ_L and is assigned to solvent restructuring in the proximity of the excited solute molecule.[61] Solvent restructuring is associated with the internal motions, like hydroxyl rotations, of solvent molecules rather than reorientation and can be described as formation of an intermolecular hydrogen bond between the excited molecule and the solvent. The long component of the correlation function has its origin in the reorganization of the solvent hydrogen bond network structure to reach an equilibrium. Matsumoto and Gubbins simulated the average lifetime for the first breaking or formation of the hydrogen bond in methanol as 0.9 ps, whereas the autocorrelation time of the hydrogen bond, which measures the time for reorganization of the solvent hydrogen bond network structure, is 11.8 ps.[59] This value is comparable to the value of τ_L of methanol (9.2 ps).[52,66] On the basis of these arguments, the ultrafast component (τ_1) determined in alcoholic solvents (e.g., the lifetimes of 1.5 and 3 ps in the case of methanol and ethanol, respectively) using the transient absorption technique can be assigned to the inertial motion of the solvent molecule involving rotation of the hydroxyl group, which is directly involved in interaction with the ketonic group of curcumin, leading to formation of an intermolecular hydrogen bond. Further, the longest component of the solvent relaxation time (in the present case, this time is given by τ_2 in Table 2) can be assigned to the reorganization of the solvent hydrogen bond network structure. This has been correlated with the longitudinal relaxation time (τ_L) of the solvent by eqs 2 and 3,[54,55]

$$\tau_2 = A(\tau_L)\exp(\Delta H/RT) \tag{2}$$

$$\ln(\tau_2) = \ln(\tau_L) + \ln(A) + \Delta H/RT \tag{3}$$

If we assume that the enthalpy of the transition state, ΔH, does not vary significantly due to change of solvents belonging to the same class, e.g., primary alcohols, we expect a linear correlation between $\ln(\tau_2)$ and $\ln(\tau_L)$ (eq 3). As shown in Figure 13A, we find a reasonably good linear correlation between these two parameters in *n*-alcohols and reconfirm the postulation that the hydrogen bond reorganization around the excited solute molecule is responsible for the dynamics of the relaxation process of the S_1 state in the alcoholic solvents observed here. This correlation also confirms that this lifetime associated with the relaxation of the S_1 state of curcumin is the property of the pure solvent and not of the excited state of the solute. Additionally, this also justifies the assignment of τ_1 and τ_2 determined from the measurement at a single wavelength, i.e., at 480 nm, to the solvation process.[60,61] Determination of $C(t)$ from the results of transient absorption measurements has been impossible because of overlap of the transient ESA and SE bands. However, close agreement between the results obtained from the measurements in methanol, ethanol, and EG using both the fluorescence and absorption techniques supports our arguments. We observe that in the case of EG, the data point shows significant deviation from the best fit line. Considering the fact that EG is a dihydric alcohol, the structure of the hydrogen-bonded complex formed between curcumin and EG is expected to be different from that formed with a normal alcohol.

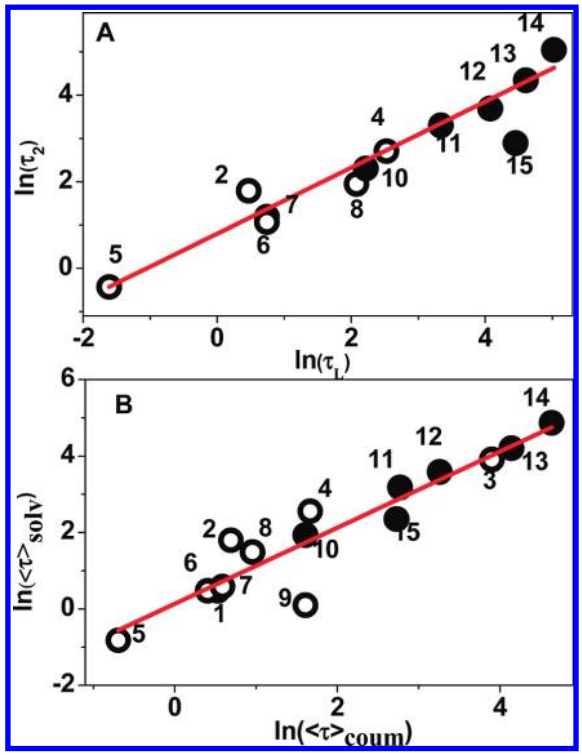

Figure 13. (A) Correlation between $\ln(\tau_2)$ and $\ln(\tau_L)$ of the solvents. The best-fit line, which represents the function $\ln(\tau_2) = 0.81 + 0.76\tau_L$ (Adj. R2 = 0.96, $N = 10$), does not include the data point for ethylene glycol. (B) Correlation between $\ln(\tau_2)$ with $\ln(\langle\tau\rangle_{avg})$ of the solvents. The best fit line represents the function: $\ln\langle\tau\rangle_{solv} = 0.81 + 0.99\langle\tau\rangle_{coum}$ (Adj. R2 = 0.86, $N = 15$), The solvents are 1,4-dioxane (1), EA (2), TA (3), BN (4), acetonitrile (5), DMF(6), DMSO(7), PC (8), formamide (9), methanol (10), ethanol (11), 1-propanol (12), 1-butanol (13), 1-pentanol (14), and ethylene glycol (15).

Figure 13A also includes the data for a few aprotic solvents for which the τ_L values are available and we find quite a good agreement between τ_2 and τ_L values of the solvents, as observed in the case of alcohols. This suggests that not only the specific hydrogen-bonding interaction as discussed above in the case of protic solvents but also the dielectric relaxation of the pure solvent play an important role in all kinds of solvents. Barbara and his co-workers made some novel measurements on the microscopic solvation dynamics of a couple of coumarin dyes or other probes, such as bianthryl, in several aprotic solvents as well as in methanol and 1-propanol.[48,62,63] Experimentally, $C(t)$ (eq 1), was well represented by a single exponential in relatively less polar solvents, such as acetone, but by a double exponential function in polar solvents.[48] Therefore, in polar solvents, $C(t)$ was fitted biexponentially to obtain two time constants (τ_a and τ_b) and the average solvation time, $\langle\tau\rangle_{solv} = a_1\tau_a + a_2\tau_b$ (where a_1 and a_2 are the corresponding amplitudes), was found to be very similar to that predicted by dielectric continuum theory.[64–66] Horng et al. also explored the intramolecular charge transfer (ICT) dynamics in a donor substituted acridinium dye in a variety of solvents and the lifetime of the charge transfer process was correlated to the average solvation time, $\langle\tau\rangle_{coum}$, which was measured with the solvation probe coumarin 153.[53,67] Solvation times of C153 were employed because they represented the best measures of the time scales of polar solvation available these days.

We have calculated $\langle\tau\rangle_{solv}$ in the polar solvents studied here using the relative amplitudes, a_1 and a_2, associated with τ_1 and τ_2, respectively, which represent the double exponential growth of transient absorption measured at 480 nm (Table 2). Our discussion on the dynamics of the S_1 state of curcumin in the alcoholic solvents clearly reveals that τ_1 and τ_2 are correlated with the bimodal solvation process. It has been shown earlier that in less polar solvents, the solvation process can be well represented by a single exponential response of the solvent.[48] Therefore, the ultrafast component, τ_v, the introduction of which was essential to obtain a good fit of the temporal profiles recorded at several wavelengths in the case of nonpolar aprotic solvents (as well as in methanol), could tentatively be assigned to the vibrational relaxation process (Table 2), considering the fact that 400 nm light excites the curcumin molecules to the higher vibrational levels of the S_1 state.[35] On the other hand, τ_2 has been approximated to the average solvation time, $\langle\tau\rangle_{solv}$. In polar solvents, τ_1 has been assigned to the inertial component of the solvent response because of close similarity of its value with that determined earlier in the corresponding solvent.[36,40] In Figure 13B, we have plotted $\ln(\langle\tau\rangle_{solv})$ vs $\ln(\langle\tau\rangle_{coum})$, and the solid line in this plot is the fit of the data collected in all kinds of solvents to follow the relation: $\ln(\langle\tau\rangle_{solv}) = 0.13 + 0.99\ \ln(\langle\tau\rangle_{coum}.)$. The near unity slope of the best fit line suggests the close similarities in the values of the average solvation time determined by us and those determined earlier to establish its correlation with the dielectric relaxation behavior of the pure solvent predicted by the dielectric continuum model.[62–67] Near unity slope of the line also suggests that the ICT process, which is responsible for the increase in dipole moment of the excited state ($\Delta\mu \sim 6.1$ D), is nearly barrierless in all kinds of solvents because of strong coupling between the local excited (LE) state and the ICT kind of the S_1 state of curcumin.[53,62,63] As a consequence of this, separation of emission into the spectra of LE and ICT states has not been possible. We have observed the emission only from the ICT kind of the S_1 state of curcumin (Figure 1B).

4.2. Deactivation of the S_1 State. Following the completion of the solvent reorganization process, the relaxed and solvated S_1-state decay to the ground electronic state by both radiative and nonradiative processes. Earlier single photon counting technique, having time resolution of about 40 ps, has been successfully used to determine the lifetime of the S_1 state in varieties of solvents.[12,14] Fluorescence decay has been fitted with either monoexponential or biexponential (or in a few cases, triexponential) functions. The lifetime obtained by monoexponential fitting for the shorter and major component in the case of multiexponential fitting has been assigned to the *cis*-enol form and the longer components with much smaller (a few percent) amplitude have been assigned to the other conformers, e.g., *trans*-diketo and some other, which has not been specified otherwise. However, the values of the lifetimes in the corresponding solvents reported in refs 12 and 14 show significant variations.

The lifetime, τ_3, given in Table 2, is assigned to the decay lifetime of the S_1 state of the *cis*-enol form in fifteen solvents. Since we have not been able to measure the lifetime longer than 500 ps and the longer decay components of transient absorption may have the contribution from the triplet state too, we will not comment on those, which are assigned to the other conformers. However, the lifetime of the *trans*-diketo conformer of curcumin has been found to be longer than 500 ps in most of the solvents studied here and hence could not be determined with reasonable accuracy (vide supra), but in 1,4-dioxane and methanol, the lifetime of this conformer has been determined to be 325 and 425 ps, respectively (Figures 6 and 11).

The value of τ_3 measured in 1,4-dioxane is very short (44 ps), and this value agrees well with that (~55 ps) reported in

another nonpolar solvent cyclohexane.[12,14] The shortest lifetime or the largest nonradiative decay rate ($\sim 15 \times 10^9$ s^{-1}) in nonpolar solvents, in which the intramolecular hydrogen bond remains undisturbed, is a direct consequence of occurrence of the ESIHT process (vide infra).[12,14] However, in more polar solvents, e.g., EA, TA, BN, acetonitrile, and PC, this lifetime becomes longer (230−300 ps), because the intramolecular hydrogen bond is perturbed by the dipole−dipole intraction.[68,69] This hypothesis can be complemented by the reduced rate of the nonradiative process ($\sim 2.5 \times 10^9$ s^{-1}).[12,14] Similar values of lifetimes in TA, PC, and acetonitrile clearly reveal the lack of viscosity dependence on the lifetime of the S_1 state of the *cis*-enol form. This excludes the possibility of occurrence of any kind of configurational relaxation in the excited state. However, the lifetimes are shorter in DMSO (175 ps) and DMF (155 ps) and the shortest (45 ps) in formamide. These three can be considered as strong hydrogen bond accepting solvents (having large β-values, Table 2),[46] which possibly disrupt the intramolecular hydrogen bond and form an intermolecular hydrogen bond not only with the enolic hydrogen but also with the phenolic hydrogens. The multiple number of intermolecular hydrogen bonds induces efficient nonradiative deactivation pathways via hydrogen stretching vibrations.[70,71] One should note that in spite of the β-value of formamide being lower than those of DMSO and DMF, the decay lifetime of curcumin in formamide is shorter than those measured in the other two solvents. However, it should also be considered that both the E_T^N value (which is a measure of both polarity and hydrogen-bonding ability of the solvent) and the α-value (~0.71, which is a measure of hydrogen bond donating ability of the solvent) of formamide are very large and these values ensure stronger hydrogen-bonding interaction between the S_1 state and formamide.[46] This explains the shortest lifetime of the S_1 state of curcumin in this solvent.

In the case of normal alcohols, τ_3 increases steadily from methanol to 1-pentanol. Because of both the hydrogen bond accepting and the donating properties of the alcohols, the solvent molecules are expected to be involved in formation of hydrogen bonds not only at the phenolic and the enolic hydrogen atoms but also with the ketonic oxygen atom, which acquire large negative charge due to intramolecular charge transfer in the excited state. Strength of the hydrogen bond between the ketonic oxygen and the alcohol molecule have been shown to become stronger with an increase in negative charge on the oxygen atom.[72] We have seen in the case of aprotic solvents that viscosity has no effect on the lifetime of the S_1 state of the *cis*-enol form. Therefore, although we find the monotonous increase of τ_3 with an increase in viscosity of the normal alcohols, this viscosity dependence cannot be explained by occurrence of configurational relaxation of the excited state. However, the hydrogen-bonding ability of the normal alcohols, given by the E_T^N value (Table 2), too varies monotonically. The E_T^N value decreases from methanol to 1-pentanol and the value of τ_3 increases with the decrease in the E_T^N value of the alcohol. This trend can only be explained by the fact that weaker hydrogen-bonding interaction between the solvent and curcumin reduces the efficiency of the nonradiative deactivation mechanism. This argument is also supported by the fact that τ_3 in EG has the value similar to that determined in methanol, in spite of its much higher viscosity than that of methanol and even that of 1-pentanol (Table 2). The E_T^N value of EG is very close to that of methanol.

4.3. Why Did Not We Observe the ESIHT Process? The role of the ESIHT process in the deactivation mechanism of the S_1 state of curcumin has repeatedly been emphasized.[12,14,16] Photoinduced ESIHT has been the subject of detailed investigations in several kinds of molecules, which have a hydrogen-bonded chelate ring as the reaction center but an asymmetric potential energy surface (PES), using different kinds of ultrafast spectroscopic techniques.[35−44] For all these kinds of molecules, a time scale of a few hundred femtoseconds has been assigned to the ESIHT process, and so far, no deuterium effect has been observed in dedicated investigations.[35,38]

Harris and co-workers reported the first investigation of the fast ESIPT reaction in 3-hydroxyflavone (3HF) using subpicosecond time-resolved stimulated emission and transient absorption spectroscopic technique and determined the ESIPT time to be 240 fs in a nonpolar solvent, methylcyclohexane (MCH).[38] In hydrogen-bonding environments, the ESPT (not ESIPT) rate changed drastically and two distinct ESPT channels were observed in methanol solution. The fast ESPT for 3HF in MeOH took place in ≤125 fs and another slow component had a lifetime of about 10 ps, which agreed well with the longitudinal relaxation time of this solvent (Table 2) and hence could be related to a solvent reorganization process. The faster ESPT time in MeOH solution has been explained by consideration of a 3HF-MeOH cyclically H-bonded 1:1 complex. The ESPT reaction coordinate in this aggregate comprises new modes resulting from hydrogen motion between the 3HF and the solvent molecules. The fast ESPT mechanism for the monosolvated 3HF could involve dual proton transfer. Lifetime of the double proton transfer reaction in 7-azaindole dimer in solution has been determined to be about 1.1 ps.[43,44]

Lochbrunner and co-workers used the ultrafast UV pump−visible probe and Elsaesser and co-workers used the ultrafast UV pump−IR probe transient absorption spectroscopic techniques to study the ESIPT of 2-(2′-hydroxyphenyl)benzothiazole (HBT) dissolved in nonpolar solvents to demonstrate that the intrinsic ESIHT is complete within 170 fs.[35,36] In 2-(2′-hydroxyphenyl)benzoxazole (HBO) too, the ESIPT reaction occurs in 170 fs and is independent of solvent or isotope.[38]

From the results of fluorescence upconversion experiments on curcumin, the component with the lifetime of about 130 ps in chloroform and 100 ps determined in methanol and EG were assigned by Adhikary et al. to the ESIHT reaction.[16] This component corresponds to that assigned to τ_3 in this work. However, we discussed earlier in section 1 of this article that the *cis*-enol conformer is a symmetric molecule with respect to the intramolecular hydrogen-bonded chelate center. In this case, the ESIHT process should be characterized by a symmetrical double-minimum potential energy surface.[68,69] Since the product of the ESIHT reaction is not different from the reactant molecule, the ultrafast spectroscopic techniques adopted here can obviously not monitor the progress of the ESIPT process in real time. In addition, the ESIHT process should be reversible in curcumin because of the low barrier between two symmetrical double minimum potential wells for the hydrogen atom transfer reaction, which were calculated earlier for molecules containing similar kind of hydrogen-bonded chelate centers.[68,69] Considering these arguments, our interpretation is at odds with the conclusions drawn by Adhikary et al. and the component τ_3, which has values varying in the range of about 40 ps to a few hundred picoseconds in different kinds of solvents, cannot be assigned to the ESIHT process. However, because of the presence of the six-membered hydrogen-bonded chelate ring, which is very similar to that present in the ESIPT molecules described above, the occurrence of ESIPT is an obvious process in the S_1 state of curcumin in nonpolar aprotic

solvent and this reaction is expected to be complete within a few hundred femtoseconds.[35–38] Since the reaction is reversible because of the low energy barrier between the reactant and the product, the excited state may be described as two rapidly interconverting structures, III and IV. The very efficient nonradiative relaxation of the S_1 state of curcumin in nonpolar solvents is the obvious manifestation of the process of interconversion by the ESIHT reaction.

However, in protic solvents, the intramolecular hydrogen bond is perturbed or broken, but an intermolecular hydrogen bond is formed during the process of hydrogen bond reorganization (also called the specific interaction via intermolecular hydrogen bonding). The hydrogen stretching vibration in this intermolecular hydrogen bond provides another efficient channel for nonradiative relaxation of the S_1 state.[70,71] However, we have observed an ultrafast component with lifetime of about 0.3 ps in methanol and we have assigned this component to vibrational relaxation process keeping an analogy to a similar component observed in aprotic solvents (Table 2). We are not sure whether this component can be assigned to the excited-state (intermolecular) hydrogen atom transfer or ESHT reaction, similar to that observed in the case of 3HF in alcohols. However, we have not been able to resolve this component in other alcohols.

5. Summary

Dynamics of the excited singlet (S_1) state of curcumin has been investigated in detail in fifteen solvents of different kinds using subpicosecond time-resolved fluorescence and absorption spectroscopic techniques. Since curcumin exists mainly as a *cis*-enol conformer in the ground state, the dynamics of the excited singlet (S_1) state of curcumin described above can be assigned to this form. This conformer is characterized by a strong intramolcular hydrogen bonding, which induces a strong nonradiative deactivation mechanism leading to shorter lifetime of this form as compared to those of other conformers. Additionally, because of the planar structure of this conformer, the S_1 state possesses a strong intramolecular charge transfer character and the dynamics of this state is dominated by the solvation process, which is multimodal and follows nonexponential dynamics. A good correlation between the longest lived component of solvation with the longitudinal relaxation time of the alcoholic solvents justifies its assignment to the hydrogen bond reorganization in the solvent hydrogen bond network structure and hence the specific hydrogen-bonding interaction between the S_1 state of curcumin and the solvent. However, we also find a good correlation between the average solvation time determined in this work in all kinds of solvents and that determined using a coumarin probe, which has already been proved to be a good marker for the dielectric continuum model, suggesting that dielectric relaxation of the pure solvent also has an important contribution in the solvation process. Although because of the presence of an intramolecular hydrogen bond in the *cis*-enol conformer, the ESIHT is an obvious process in the excited state, two spectroscopic techniques applied here do not allow us to monitor it in real time. However, its signature is clearly evident in the shorter lifetime of the S_1 state in nonpolar aprotic solvents, in which the intramolecular hydrogen bond remains nearly unperturbed. In polar solvents the intramolecular hydrogen bond is disturbed, leading to the reduced efficiency of the nonradiative deactivation mechanism. However, in protic solvents, the intermolecular hydrogen-bonding interaction between curcumin and the solvent provides another efficient channel for nonradiative deactivation mechanism of the S_1 state.

Acknowledgment. We are grateful to Prof. Anindya Datta of IIT Bombay for his kind help in performing the fluorescence upconversion experiments in his laboratory. Dr. K. I. Priyadarsini, RPCD, for providing purified samples of curcumin and Dr. S. K. Sarkar, Head, RPCD, BARC, and Dr. T. Mukherjee, Director, Chemistry Group, BARC, for their constant encouragements.

Supporting Information Available: Figures of absorbance−time profiles. This material is available free of charge via the Internet at http://pubs.acs.org.

References and Notes

(1) Aggarwal, B. B.; Sundaram, C.; Malini, N.; Ichikawa, H. In *Molecular Targets and Therapeutic uses of curcumin in health and disease*; Aggarwal, B. B., Surth, Y. J., Eds.; Springer: New York, 2007.
(2) Srimal, R. C.; Dhawan, B. N. *J. Pharm. Pharmacol.* **1973**, *25*, 447.
(3) Sharma, O. P. *Biochem. Pharmacol.* **1976**, *2*, 5–1811.
(4) Singh, S.; Aggarwal, B. B. *J. Biol. Chem.* **1995**, *270*, 24995.
(5) Goel, A.; Kannumakkara, A. B.; Aggarwal, B. B. *Biochem. Pharamacol.* **2008**, *75*, 787.
(6) Lantz, R. C.; Chen, G. J.; Solyom, A. M.; Jolad, S. D.; Timmerman, B. M. *Phytomedicine* **2005**, *12*, 445.
(7) Aggarwal, B. B.; Kumar, A.; Bharti, A. C. *Anticancer Res.* **2003**, *23*, 363.
(8) Anand, P.; Thomas, S. G.; Kunnumakkara, A. B.; Sundaram, C.; Kuzhuvelil, B. H.; Sung, B.; Tharakan, S. T.; Aggarwal, B. B. *Biochem. Phramacol.* **2008**, *76*, 1590.
(9) Yang, F.; Lim, G. P.; Begum, A. N.; Ubeda, O. J.; Simmons, M. R.; Ambegaonkar, S. S.; Chen, P. P.; Kayed, R.; Glabe, C. G.; Frautschy, S. A.; Cole, G. M. *J. Biol. Chem.* **2005**, *280*, 5892.
(10) Masuda, M.; Suzuki, N.; Taniguchi, S.; Oikawa, T.; Nonaka, T.; Iwatsubo, T.; Hisangav, S.-i.; Goedert, M.; Hasegawa, M. *Biochemistry* **2006**, *45*, 6085.
(11) Gorman, A. A.; Hamblett, I.; Srinivasan, V. S.; Wood, P. D. *Photochem. Photobiol.* **1994**, *59*, 389.
(12) Khopde, S. M.; Priyadarsini, K. I.; Palit, D. K.; Mukherjee, T. *Photochem. Photobiol.* **2000**, *72*, 625.
(13) (a) Priyadarsini, K. I. *Free Rad. Chem. Biol.* **1997**, *23*, 838. (b) Barik, A.; Priyadarsini, K. I.; Mohan, H. *Orient. J. Chem.* **2002**, *18*, 427. (c) Priyadarsini, K. I.; Maity, D. K.; Naik, G. H.; Kumar, M. S.; Unnikrishnan, M. K.; Satav, J. G.; Mohan, H. *Free Rad. Chem. Biol.* **2003**, *35*, 475. (d) Priyadarsini, K. I. *J. Photochem. Photobiol. C.* **2009**, *10*, 81.
(14) (a) Nardo, L.; Paderno, R.; Andreoni, A.; Masson, M.; Haukvik, T.; Tonnesen, H. H. *Spectroscopy* **2008**, *22*, 187. (b) Nardo, L.; Andreoni, A.; Bondani, M.; Masson, M.; Tonnesen, H. H. *J. Photochem. Photobiol. B: Biol.* **2009**, *97*, 77.
(15) Caselli, M.; Ferrari, E.; Imbriano, C.; Pignedoli, F.; Saladini, M.; Ponterini, G. *J. Photochem. Photobiol. A: Chem.* **2010**, *210*, 115.
(16) Adhikary, R.; Mukherjee, P.; Kee, T. W.; Petrich, J. W. *J. Phys. Chem. B* **2009**, *113*, 5255.
(17) Adhikary, R.; Carlson, P. J.; Kee, T. W.; Petrich, J. W. *J. Phys. Chem. B* **2010**, *114*, 2997.
(18) Dahl, T. A.; Bilski, P.; Reszka, K. J.; Chignell, C. F. *Photochem. Photobiol.* **1994**, *59*, 290.
(19) Chignell, C. F.; Bilski, P.; Reszka, K. J.; Motten, A. G.; Sik, R. H.; Dahl, T. A. *Photochem. Photobiol.* **1994**, *59*, 295.
(20) Sun, Y. M.; Wang, R. X.; Yuan, S. L.; Lin, X. J.; Liu, C. B. *Chineese J. Chem.* **2004**, *22*, 827.
(21) Balasubramanian, K. *J. Agric. Food Chem.* **2006**, *54*, 3512.
(22) Barclay, L. R.; Vinquist, M. R.; Mukai, K.; Goto, H.; Hashimoto, Y.; Tokunaga, A.; Uno, H. *Org. Lett.* **2000**, *2*, 2841.
(23) Payton, F.; Sandusky, P.; Alworth, W. L. *J. Nat. Prod.* **2007**, 143.
(24) Roughley, P. J.; Whiting, D. A. *J. Chem. Soc., Perkin Trans. I* **1973**, *20*, 2379.
(25) Matthes, H. W. D.; Luu, B.; Ourisson, G. *Photochemistry* **1980**, *170*, 425.
(26) Pedersen, U.; Rasmussen, P. B.; Lawesson, S.-O. *Liebigs Ann. Chem.* **1985**, *8*, 1557.
(27) Bong, P.-H. *Bull. Korean Chem. Soc.* **2000**, *21*, 81.
(28) Shen, L.; Ji, H.-F. *Spectrochim. Acta, Part A* **2007**, *67*, 619.
(29) Shen, L.; Zhang, H. Y.; Ji, H.-F. *Org. Lett.* **2005**, *7*, 243.
(30) Kong, L.; Priyadarsini, K. I.; Zhang, H. Y. *J. Mol. Struct. THEOCHEM* **2004**, *688*, 111.
(31) Sun, Y. M.; Zhang, H. Y.; Chen, D. Z.; Liu, C. B. *Org. Lett.* **2002**, *4*, 2909.
(32) Wright, J. S. *J. Mol. Struct. THEOCHEM* **2002**, *591*, 207.
(33) Maroncelli, M.; Fleming, G. R. *J. Chem. Phys.* **1987**, *86*, 6221.
(34) Cross, A. J.; Fleming, G. R. *Biophys. J.* **1984**, *46*, 45.

(35) (a) Elsaesser, T. In *Femtosecond Chemistry*; Manz, J., Wöste, L., Eds.; VCH-Verlag: Weinheim, Germany, 1995; Vol. 2; pp 563−579. (b) Elsaesser, T.; Kaiser, W. *Chem. Phys. Lett.* **1986**, *128*, 231. (c) Laermer, F.; Elsaesser, T.; Kaiser, W. *Chem. Phys. Lett.* **1988**, *148*, 119. (d) Frey, W.; Laermer, F.; Elsaesser, T. *J. Phys. Chem.* **1991**, *95*, 10391.

(36) (a) Lochbrunner, S.; Wurzer, A. J.; Riedle, E. *J. Phys. Chem. A* **2003**, *107*, 10580. (b) Lochbrunner, S.; Schultz, T.; Schmitt, M.; Shaffer, J. P.; Zgierski, M. Z.; Stolow, A. *J. Chem. Phys.* **2001**, *114*, 2519. (c) Lochbrunner, S.; Szeghalmi, A.; Stock, K.; Schmitt, M. *J. Chem. Phys.* **2005**, *122*, 244315. (d) Lochbrunner, S.; Wurzer, A. J.; Riedle, E. *J. Phys. Chem.* **2003**, *107*, 10580. (e) de Vivie-Riedle, R.; De Waele, V.; Kurtz, L.; Riedle, E. *J. Phys. Chem.* **2003**, *107*, 10591. (f) Stock, K.; Bizjak, T.; Lochbrunner, S. *Chem. Phys. Lett.* **2002**, *354*, 409. (g) Lochbrunner, S.; Schultz, T.; Schmitt, M.; Shaffer, M.; Zgierski, M. Z.; Stolow, A. *J. Chem. Phys.* **2001**, *114*, 2519. (h) Lochbrunner, S.; Wurzer, A. J.; Riedle, E. *J. Chem. Phys.* **2000**, *112*, 10699.

(37) Abou-Zeid, O. K.; Jimnez, R.; Thompson, E. H. Z.; Millar, D. P.; Romesberg, F. E. *J. Phys. Chem. A* **2002**, *106*, 3665.

(38) Schwartz, B. J.; Peteanu, L. A.; Harris, C. B. *J. Phys. Chem.* **1992**, *96*, 3591.

(39) Ormoson, S. M.; LeGourrierec, D.; Brown, R. G.; Foggi, P. *J. Chem. Soc., Chem. Commun.* **1995**, 2133.

(40) Douhal, A.; Lahmani, F.; Zewail, A. H. *Chem. Phys.* **1996**, *207*, 477.

(41) Huston, A. L.; Scott, G. W.; Gupta, A. *J. Chem. Phys.* **1982**, *76*, 4978.

(42) Arthen-Engeland, Th.; Bultmann, T.; Ernsting, N. P.; Rodriguez, M. A.; Thiel, W. *Chem. Phys.* **1992**, *163*, 43.

(43) Takeuchi, S.; Tahara, T. *Proc. Natl. Acad. Sci. U.S.A.* **2007**, *104*, 5285.

(44) Share, P.; Pereira, M.; Sarisky, M.; Repinec, S.; Hochstrasser, R. M. *J. Lumin.* **1991**, *48 & 49*, 204.

(45) Burai, T. N.; Mukherjee, T. K.; Lahiri, P.; Datta, A. *J. Chem. Phys.* **2009**, *131*, 34504.

(46) Reicherdt, C. *Solvents and Solvent Effects in Organic Chemistry*; VCH: Weinheim, 1990.

(47) Horng, M. L.; Gardeki, J. A.; Papazyan, A.; Maroncelli, M. *J. Phys. Chem.* **1995**, *99*, 17311.

(48) Jarzeba, W.; Walker, G. C.; Johnson, A. E.; Barbara, P. F. *Chem. Phys.* **1991**, *152*, 57.

(49) Nibbering, E. T. J.; Fidder, H.; Pines, E. *Annu. Rev. Phys. Chem.* **2005**, *56*, 337.

(50) Nibbering, E. T. J.; Elsaesser, T. *Chem. Rev.* **2004**, *104*, 1887.

(51) Martini, I.; Hartland, G. V. *J. Phys. Chem.* **1996**, *100*, 19764.

(52) Harju, T. O.; Huizer, A. H.; Varma, C. A. G. O. *Chem. Phys.* **1995**, *200*, 215.

(53) Horng, M. L.; Dahl, K.; Jones, G., II; Maroncelli, M. *Chem. Phys. Lett.* **1999**, *315*, 363.

(54) Yu, J.; Berg, M. *Chem. Phys. Lett.* **1993**, *208*, 315.

(55) Benigno, A. J.; Ahmed, E.; Berg, M. *J. Chem. Phys.* **1996**, *104*, 7382.

(56) (a) Samant, V.; Singh, A. K.; Ramakrishna, G.; Ghosh, H. N.; Ghanty, T.; Palit, D. K. *J. Phys. Chem. A* **2005**, *109*, 8693. (b) Varne, M.; Samant, V.; Mondal, J.; Nayak, S. K.; Ghosh, H. N.; Palit, D. K. *Chem. Phys. Chem.* **2009**, *10*, 2979. (c) Mondal, J. A.; Samant, V.; Varne, M.; Singh., A. K.; Ghanty, T. K.; Ghosh, H. N.; Palit, D. K. *Chem. Phys. Chem.* **2009**, *10*, 2995.

(57) Garg, S. K.; Smyth, C. P. *J. Phys. Chem.* **1965**, *69*, 129.

(58) Bertolini, D.; Cassattari, M.; Salvetti, G. *J. Chem. Phys.* **1982**, *76*, 325.

(59) Matsumoto, M.; Gubbins, K. *J. Chem. Phys.* **1990**, *93*, 1981.

(60) Kovalenko, S. A.; Ernsting, N. P.; Ruthmann, J. *J. Chem. Phys.* **1997**, *106*, 3504.

(61) Nagarajan, V.; Bearley, A. M.; Kang., T. J.; Barbara, P. F. *J. Chem. Phys.* **1987**, *86*, 3183.

(62) Kang, T. J.; Kahlow, M. A.; Giser, D.; Swallen, S.; Nagarajan, V.; Jarzeba, W.; Barbara, P. F. *J. Phys. Chem.* **1988**, *92*, 6800.

(63) Kang, T. J.; Jarzeba, J.; Barbara, P. F.; Fonseca, T. *Chem. Phys.* **1990**, *149*, 81.

(64) Kivelsion, D.; Madden, P. A. *Annu. Rev. Phys. Chem.* **1980**, *31*, 583.

(65) Frohlich, H. *Theory of Dielectrics*; Oxford University Press: Oxford, U.K., 1949.

(66) Simon, J. D. *Acc. Chem. Res.* **1988**, *21*, 128.

(67) Maroncelli, M. *Chem. Phys.* **1997**, *106*, 1545. Maroncelli, M. *J. Mol. Liq.* **1993**, *57*, 1.

(68) Barbara, P. F.; Walsh, P. K.; Brus, L. E. *J. Phys. Chem.* **1989**, *93*, 29.

(69) Rossetti, R.; Haddon, R. C.; Brus, L. E. *J. Am. Chem. Soc.* **1980**, *102*, 6913.

(70) Palit, D. K.; Pal, H.; Mukherjee, T.; Mittal, J. P. *J. Chem. Soc., Faraday Trans.* **1990**, *86*, 3861.

(71) Folm, S. R.; Barbara, P. F. *J. Phys. Chem.* **1985**, *89*, 4489.

(72) (a) Zhao, G.; Han, K. *J. Phys. Chem. A* **2007**, *111*, 2469. (b) Zhao, G. J.; Han, K. *J. Phys. Chem. A* **2007**, *111*, 9218. (c) Zhao, G.; Kan., K. *Chem. Phys. Chem* **2008**, *9*, 1842. (d) Zhao, G.; Kan., K. *J. Comput. Chem.* **2008**, *29*, 2010.

JP1038249